Synthesis and photophysical properties of 1,7-aroyl BODIPYs: An experimental and theoretical study

Ilya V. Efimov,*[a] Almira R. Miftyakhova,[a] Maria D. Matveeva,[b] Dmitry I. Zhilyaev,[a] Paweł Czulkin,[c] Patryk Janasik,[c] Giovanni Talarico*[d] and Leonid G. Voskressensky[a]

[a] *Research Center: Molecular Design and Synthesis of Innovative Compounds for Medicine, RUDN University, 117198, Russia, Moscow, Miklukho-Maklaya st, 6*

[b] *A.V. Topchiev Institute of Petrochemical Synthesis, Russian Academy of Sciences, Leninsky pr. 29, 119991, Moscow, Russian Federation*

[c] *Department of Physical Chemistry and Technology of Polymers, Faculty of Chemistry, Silesian University of Technology, Strzody 9,44-100 Gliwice, Poland*

[d] *Dipartimento di Scienze Chimiche, Università di Napoli Federico II, Via Cintia, 80126 Napoli, Italy*

* *Corresponding author. E-mail address: ilya.efimov00@gmail.com*

Supporting information

Table of Contents

1. NMR spectra for products

^{1}H NMR spectrum of **4a**

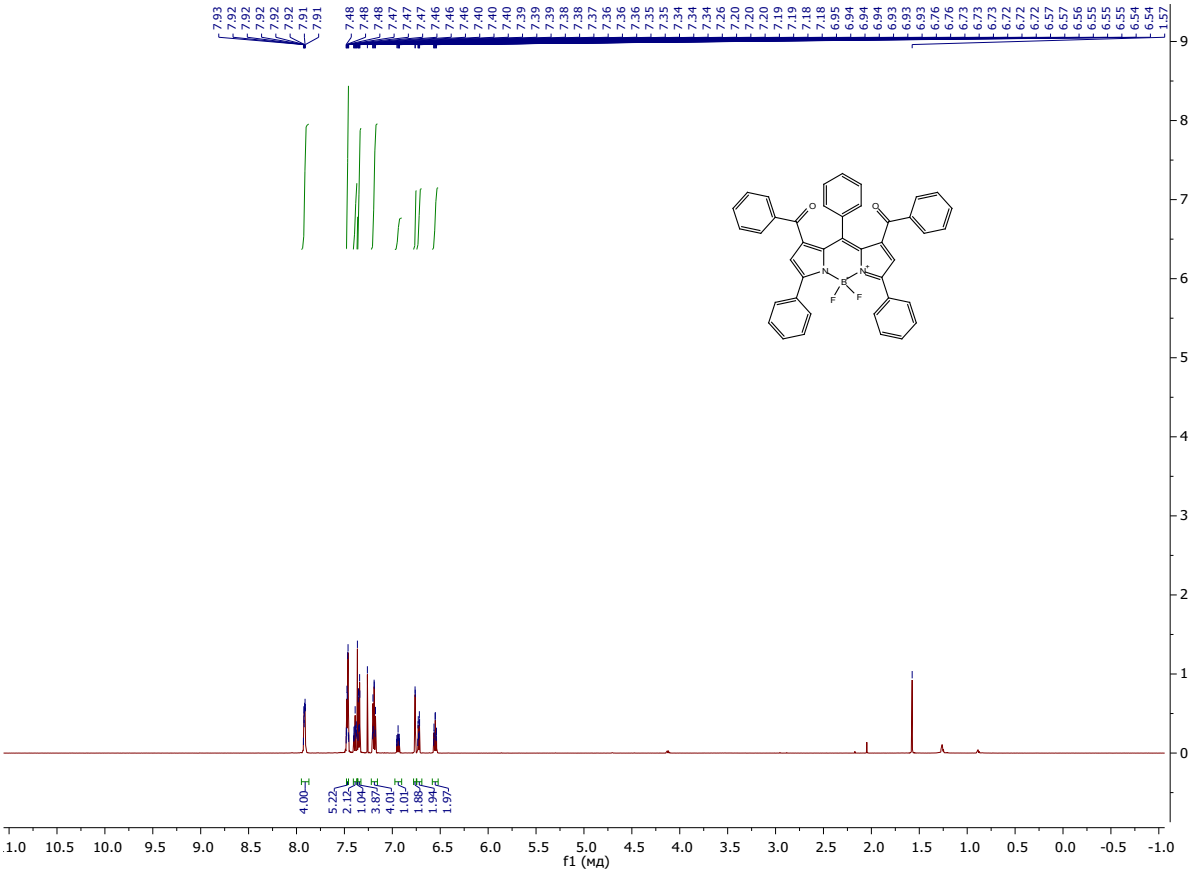

^{13}C NMR spectrum of **4a**

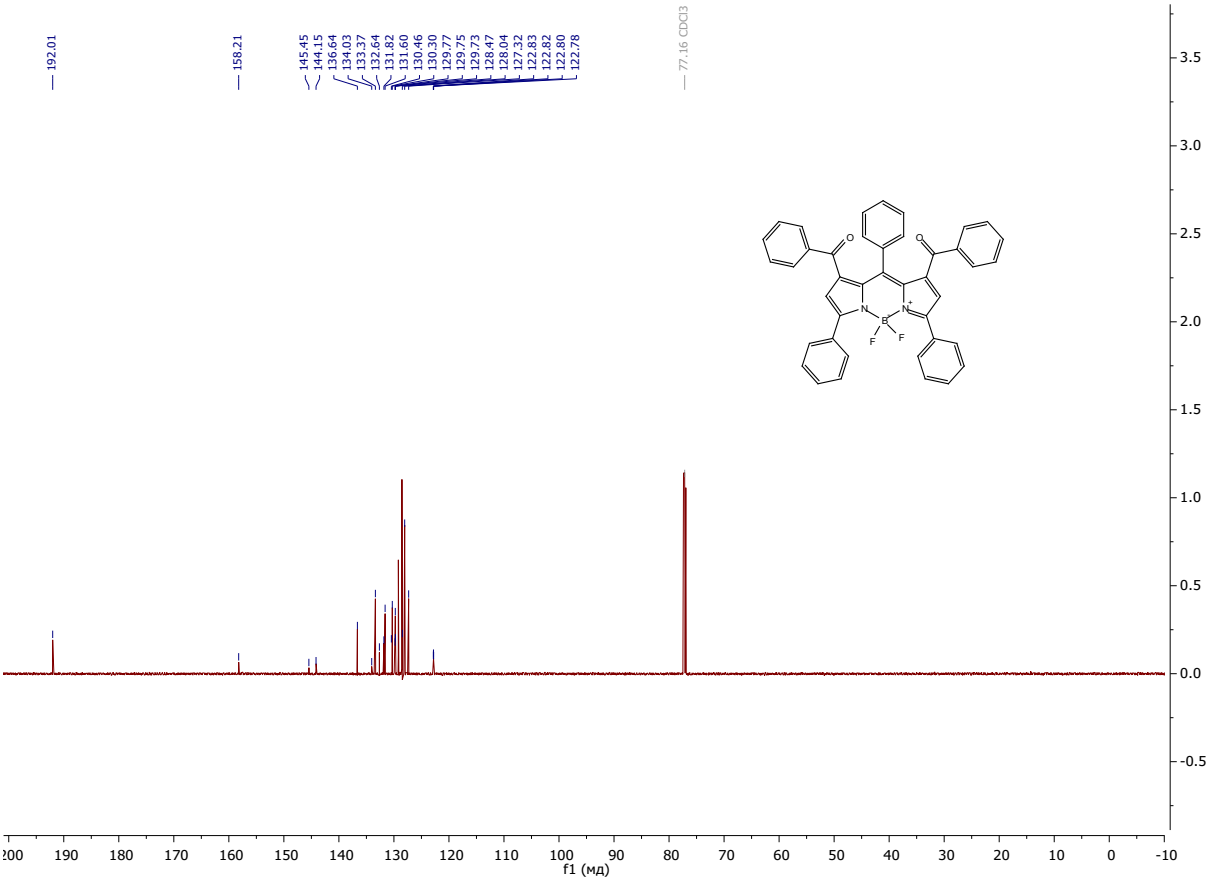

^{19}F NMR spectrum of **4a**

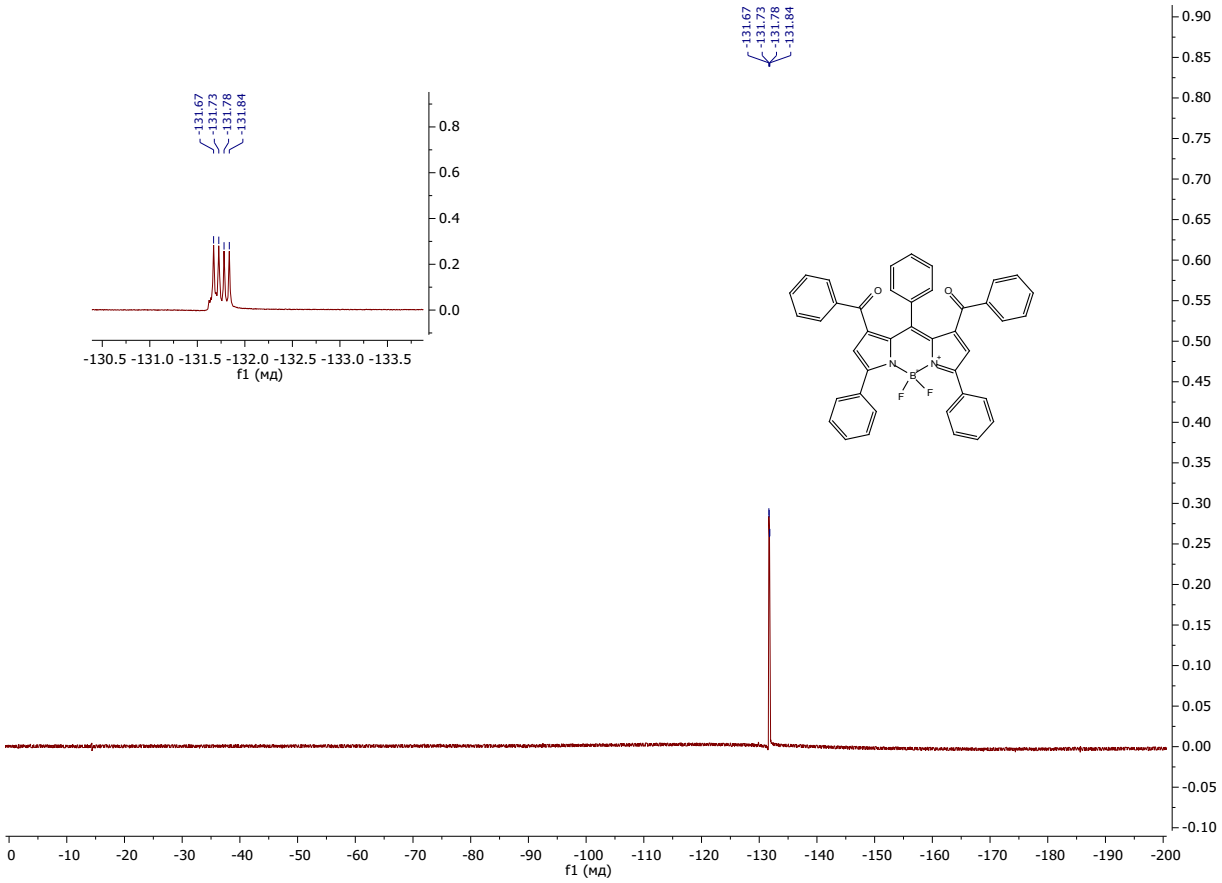

^{1}H NMR spectrum of **4b**

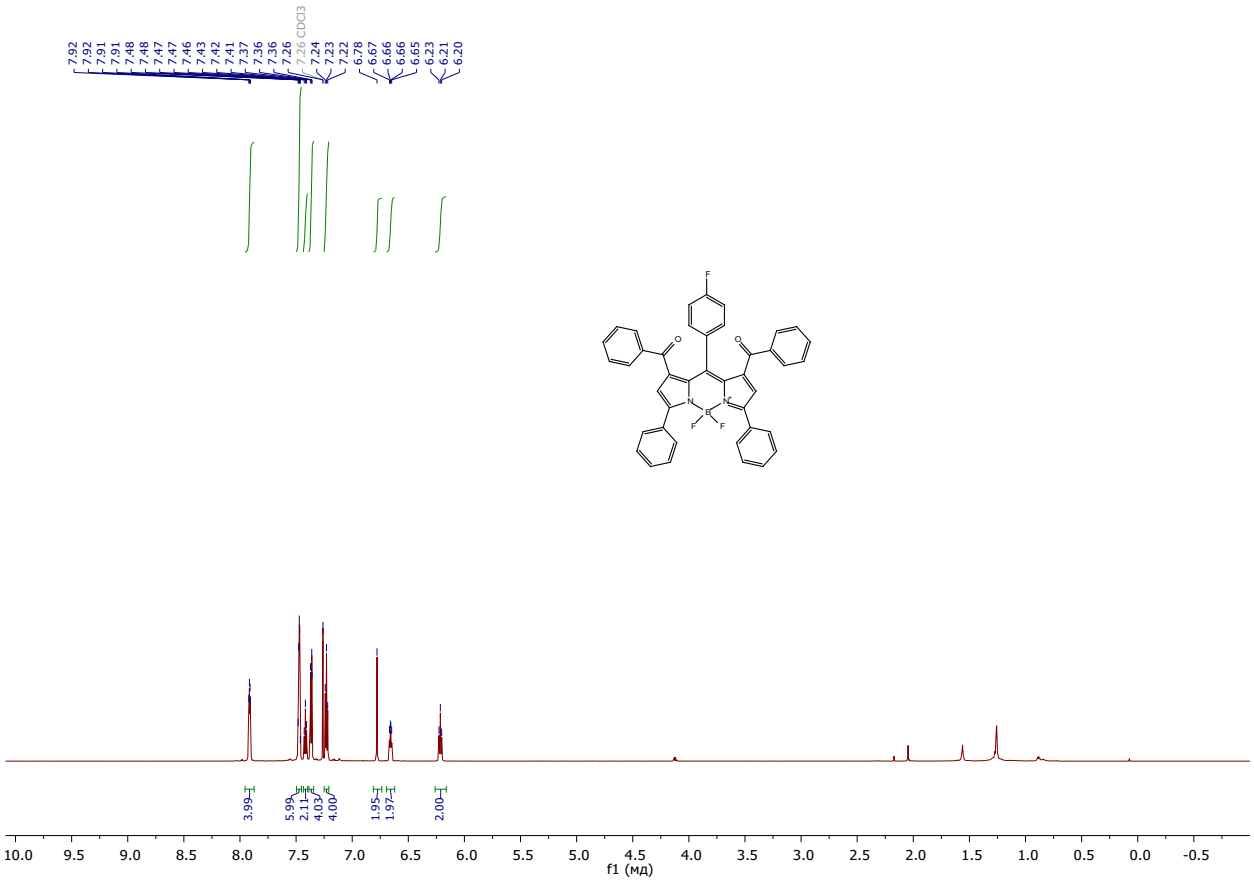

^{13}C NMR spectrum of **4b**

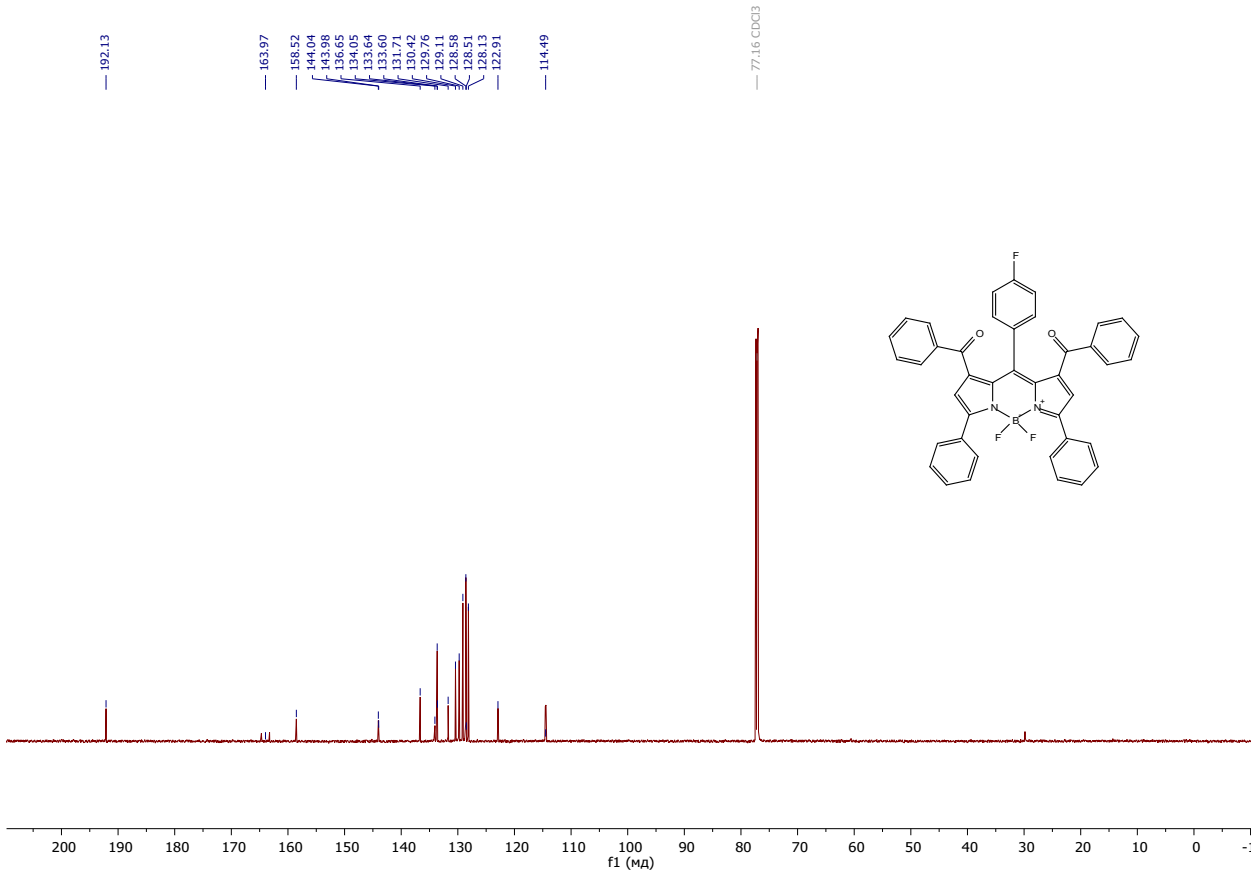

^{19}F NMR spectrum of 4**b**

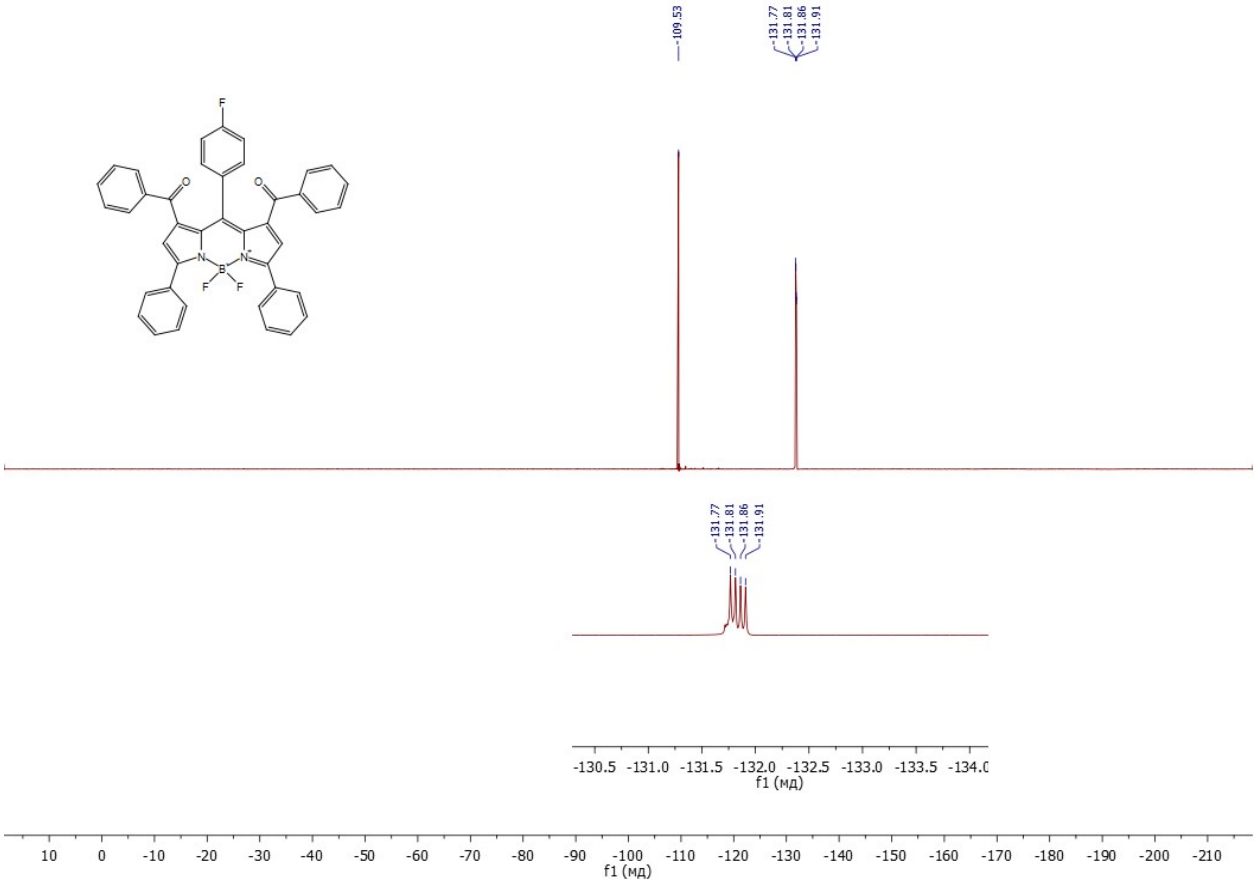

[1]H NMR spectrum of **4c**

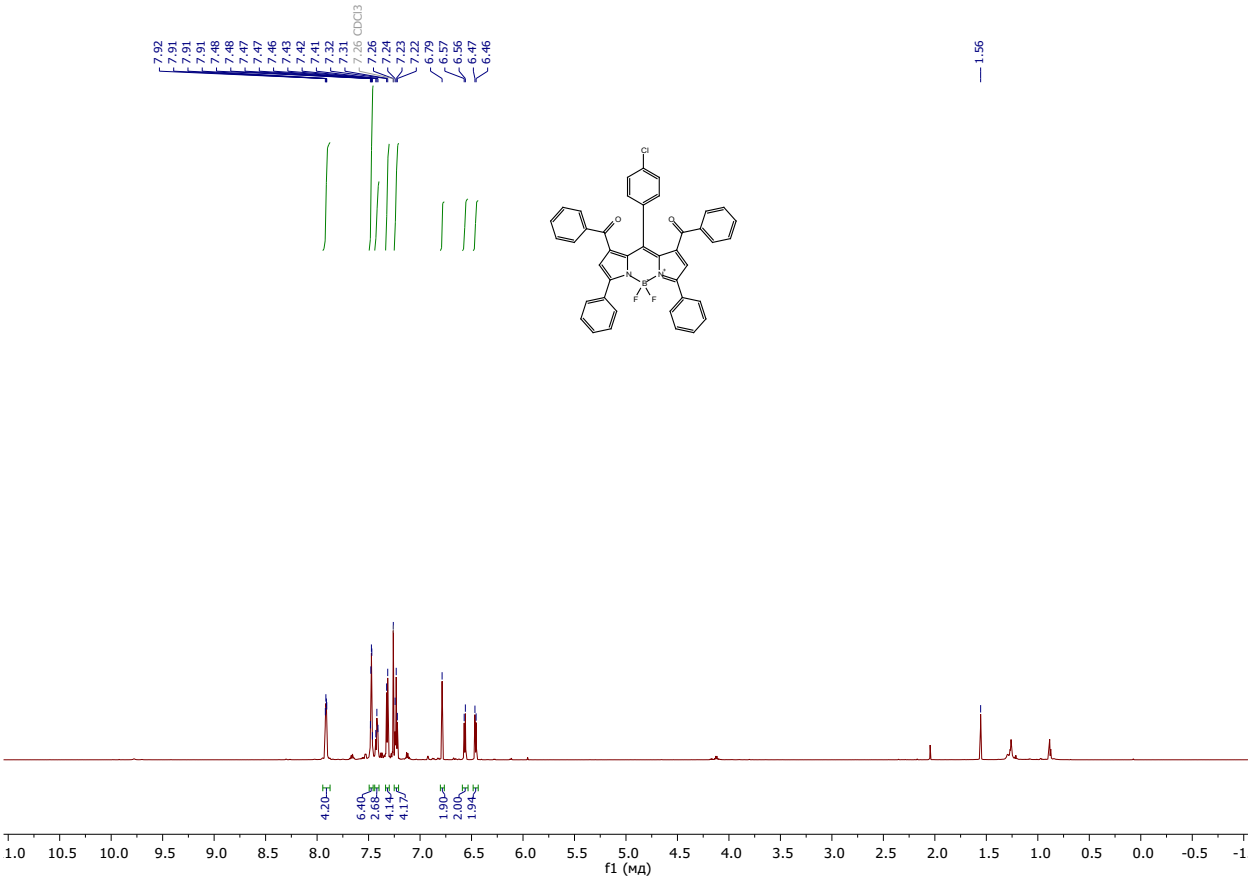

[13]C NMR spectrum of **4c**

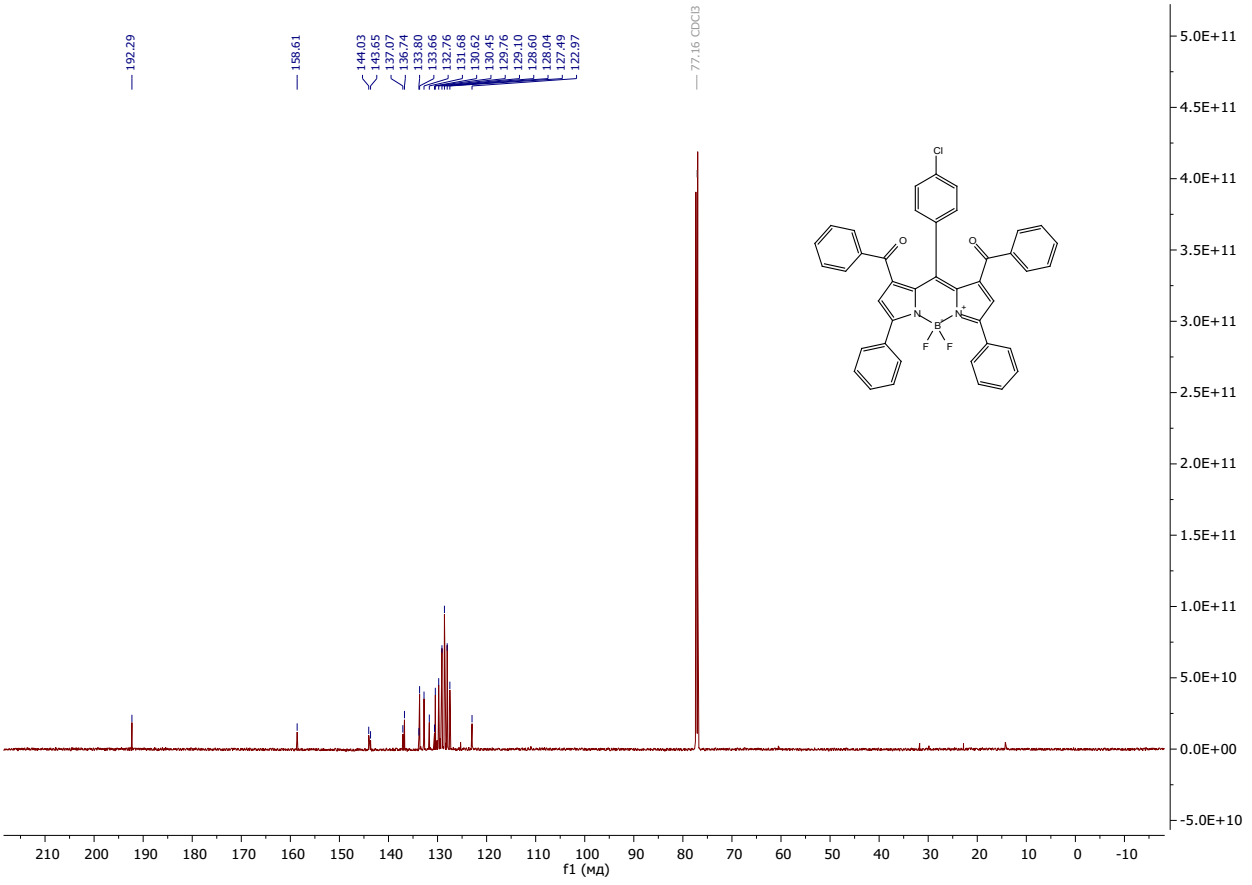

^{19}F NMR spectrum of **4c**

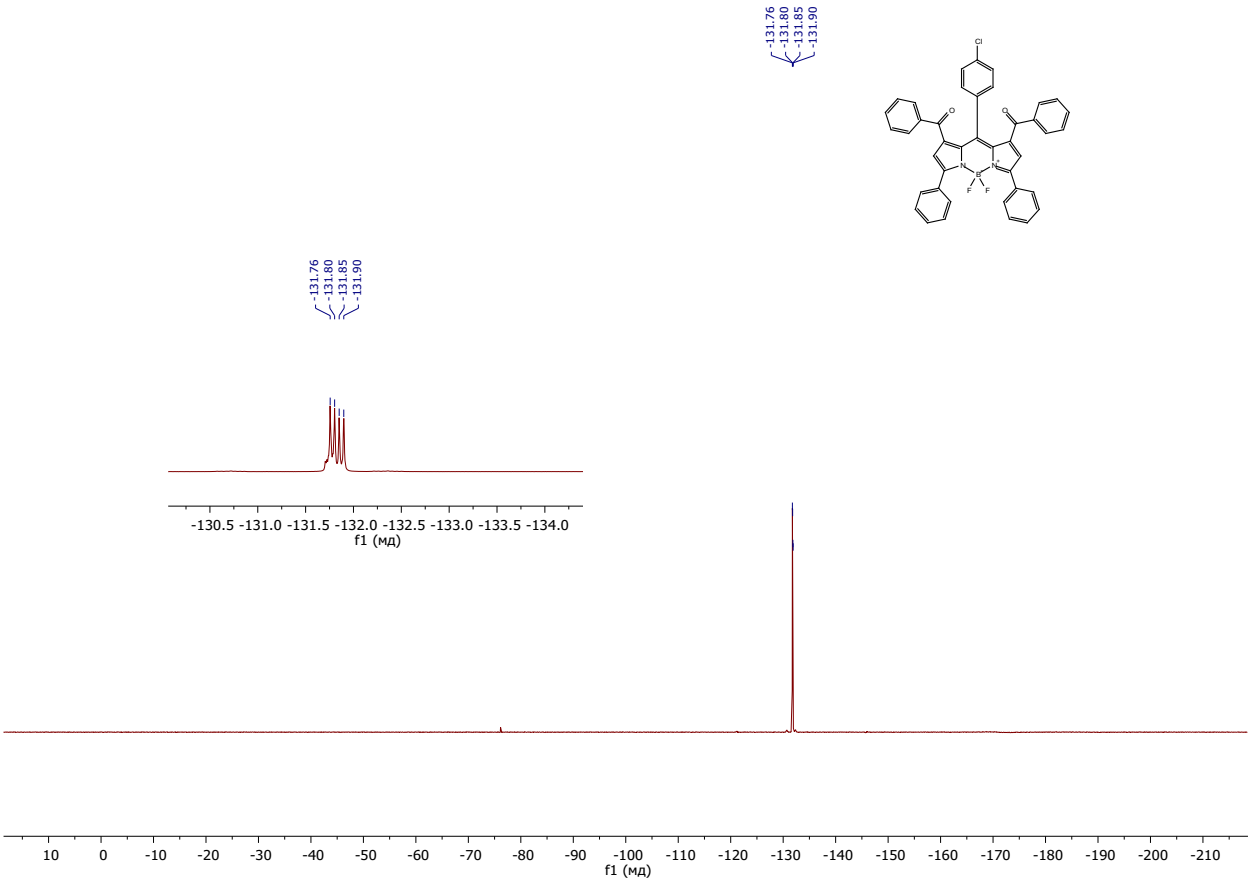

^{1}H NMR spectrum of **4d**

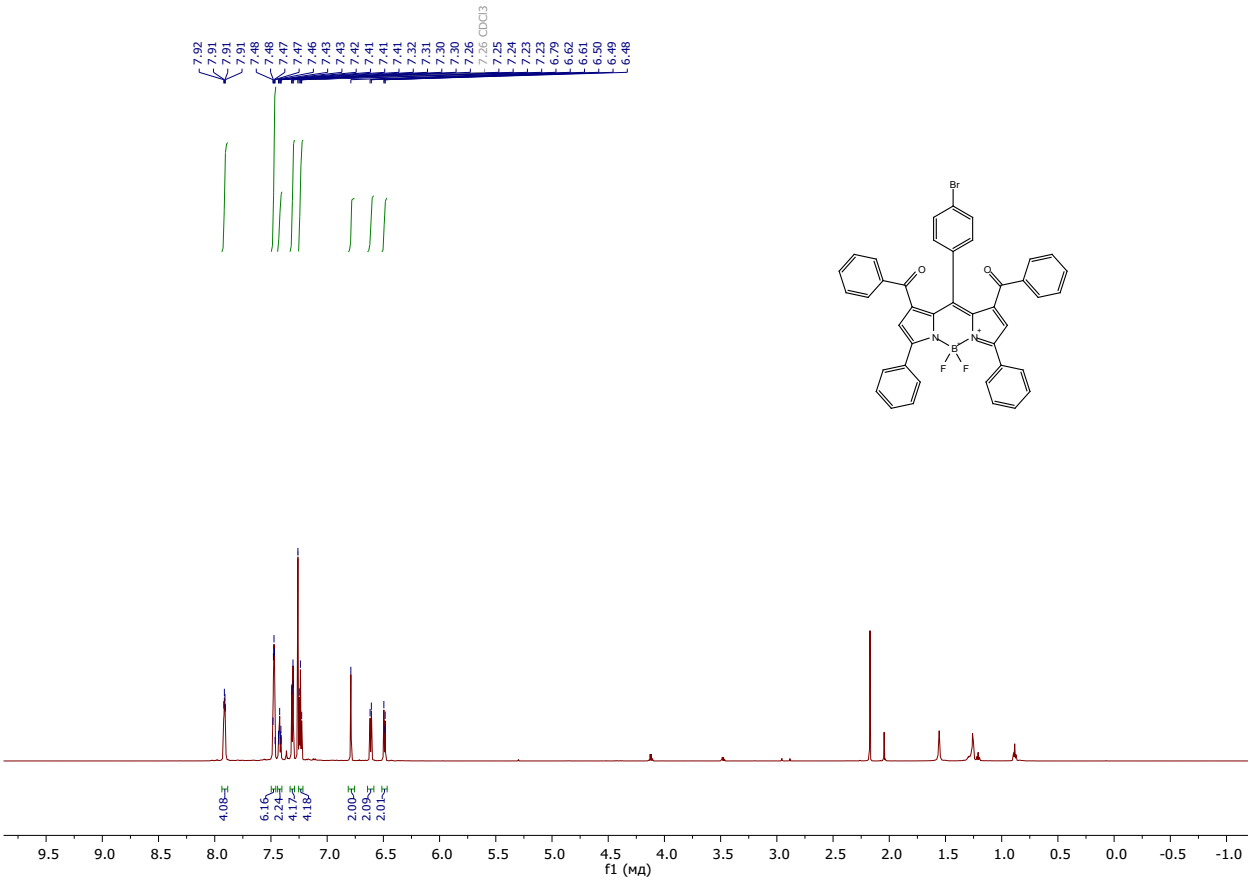

^{13}C NMR spectrum of **4d**

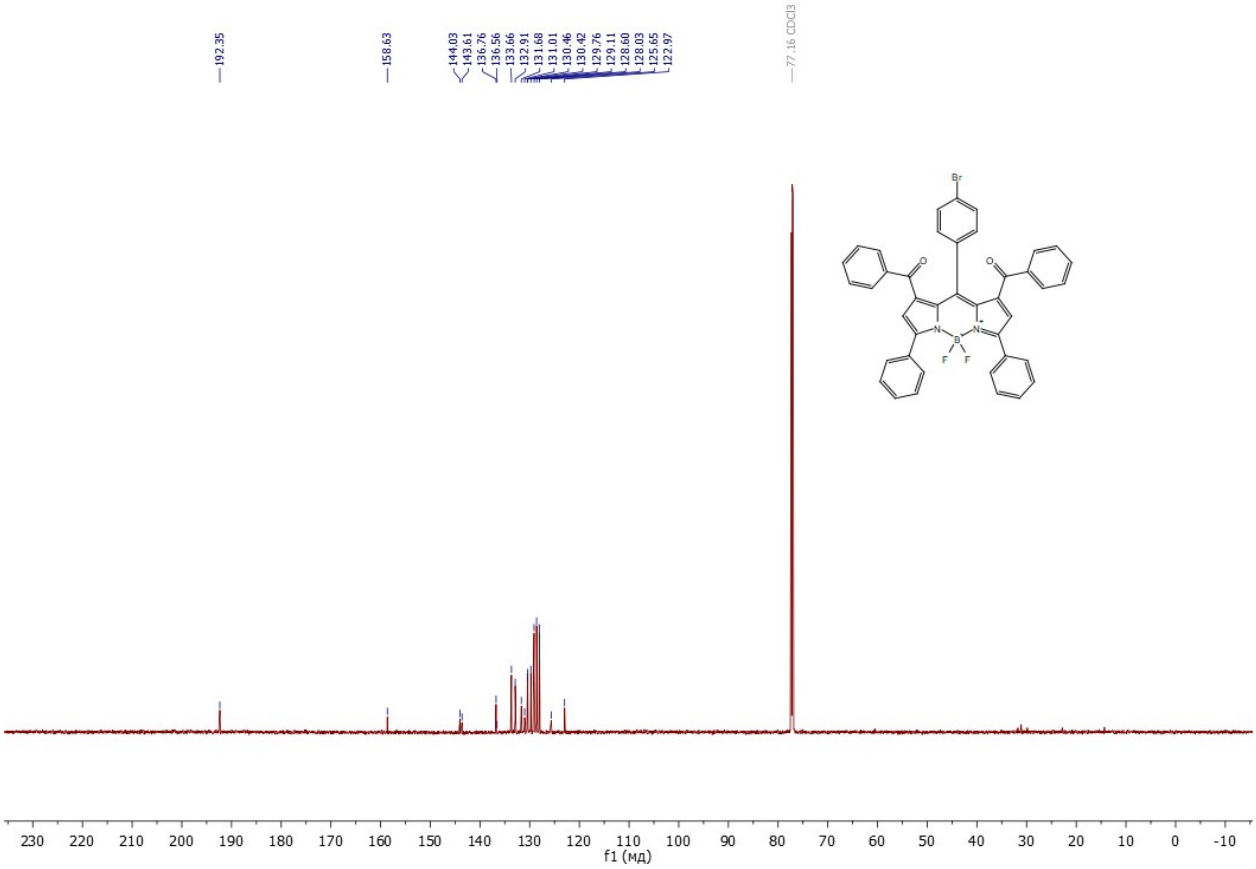

^{19}F NMR spectrum of **4d**

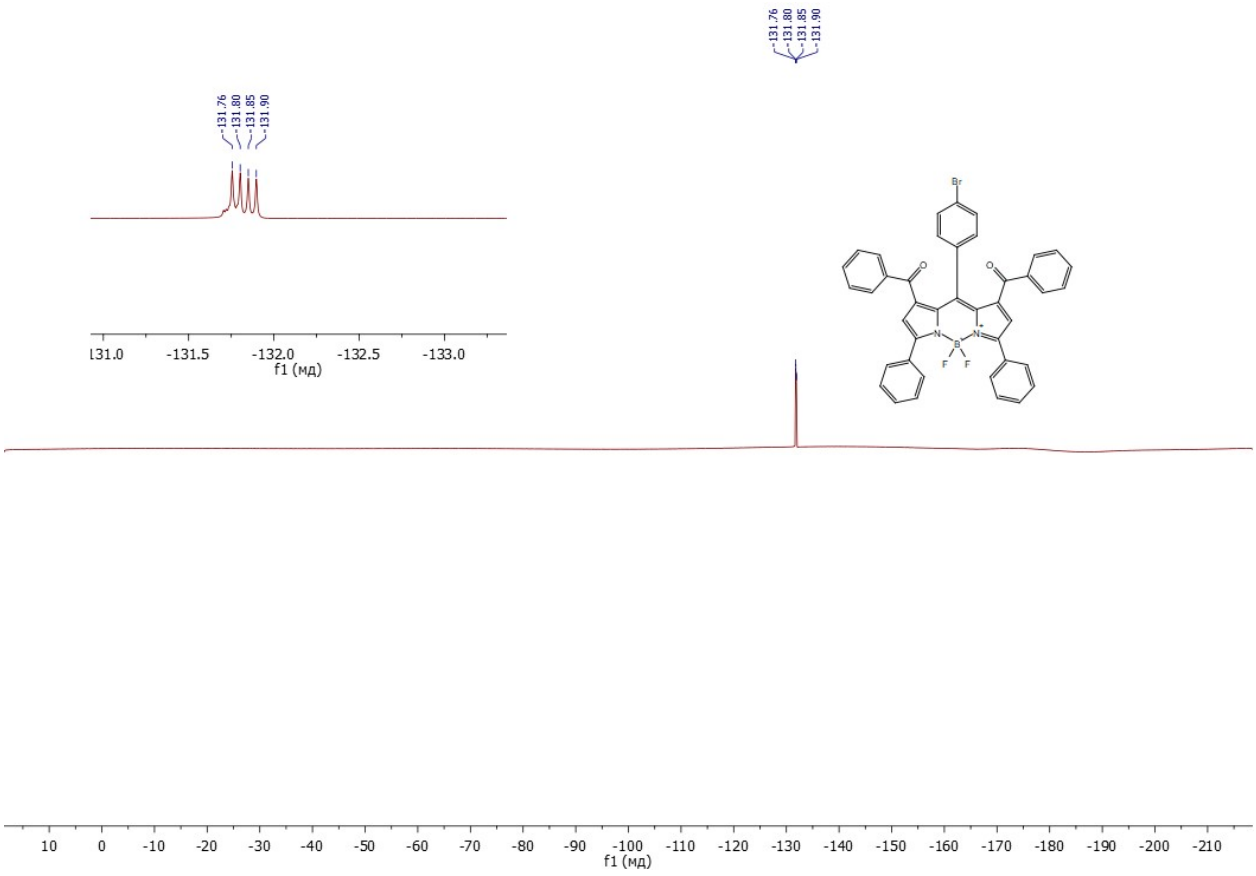

^{1}H NMR spectrum of **4e**

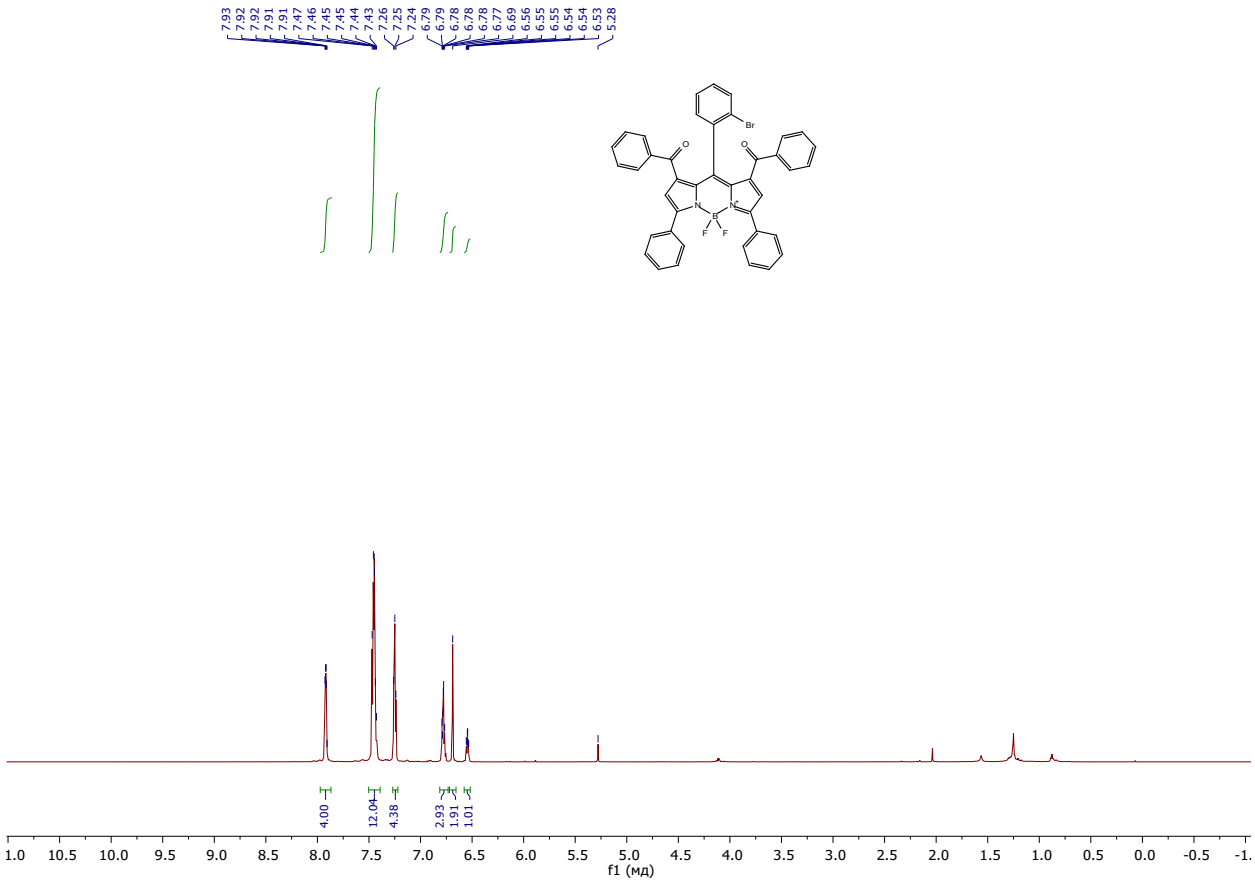

^{13}C NMR spectrum of **4e**

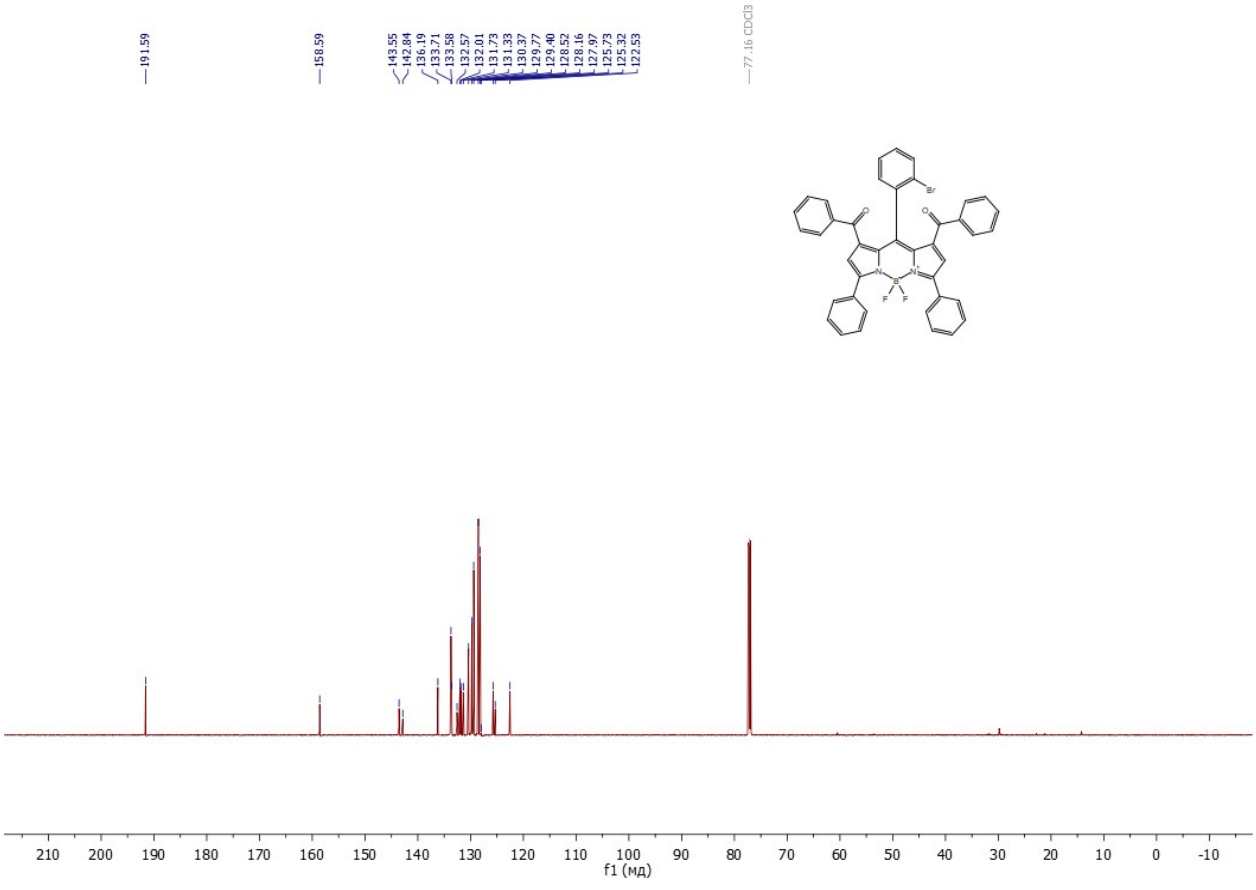

^{19}F NMR spectrum of **4e**

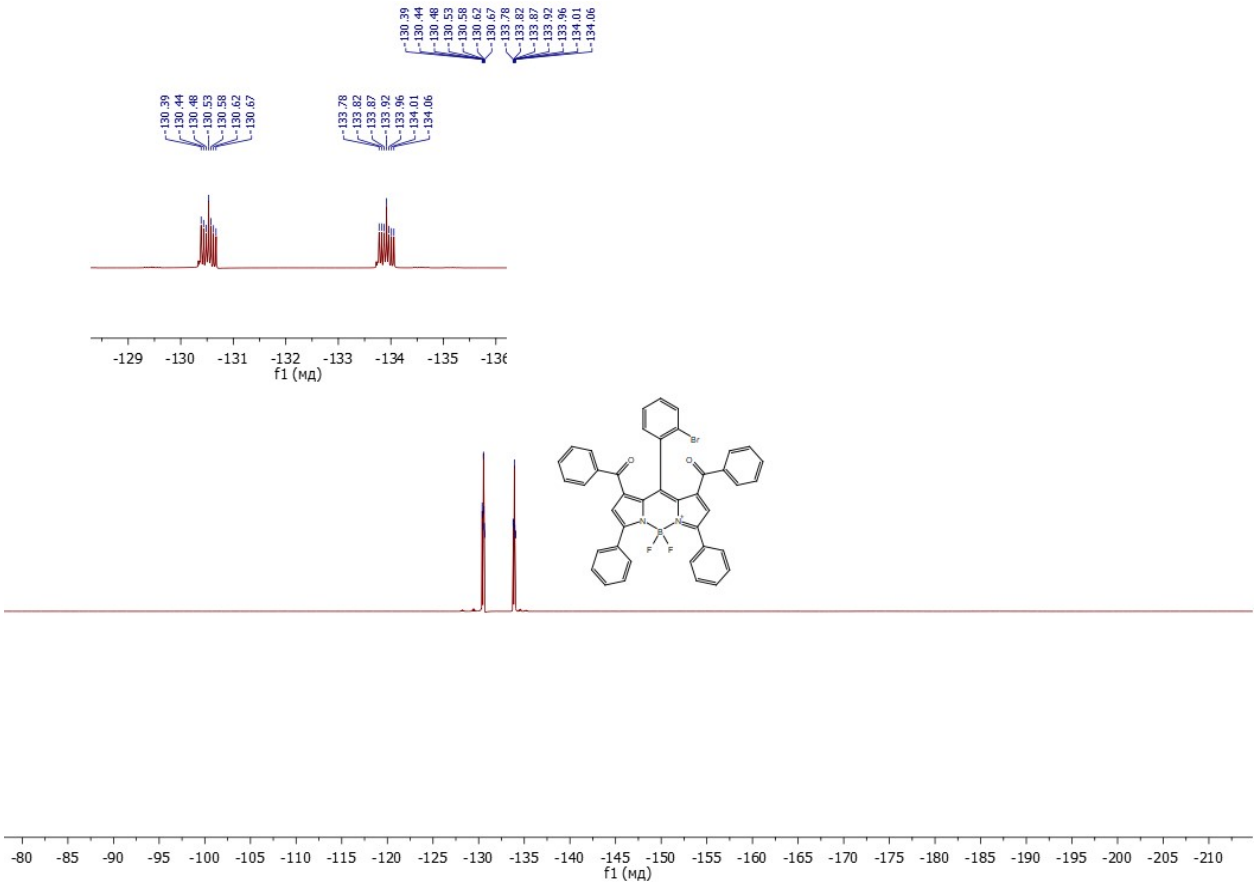

^{1}H NMR spectrum of **4f**

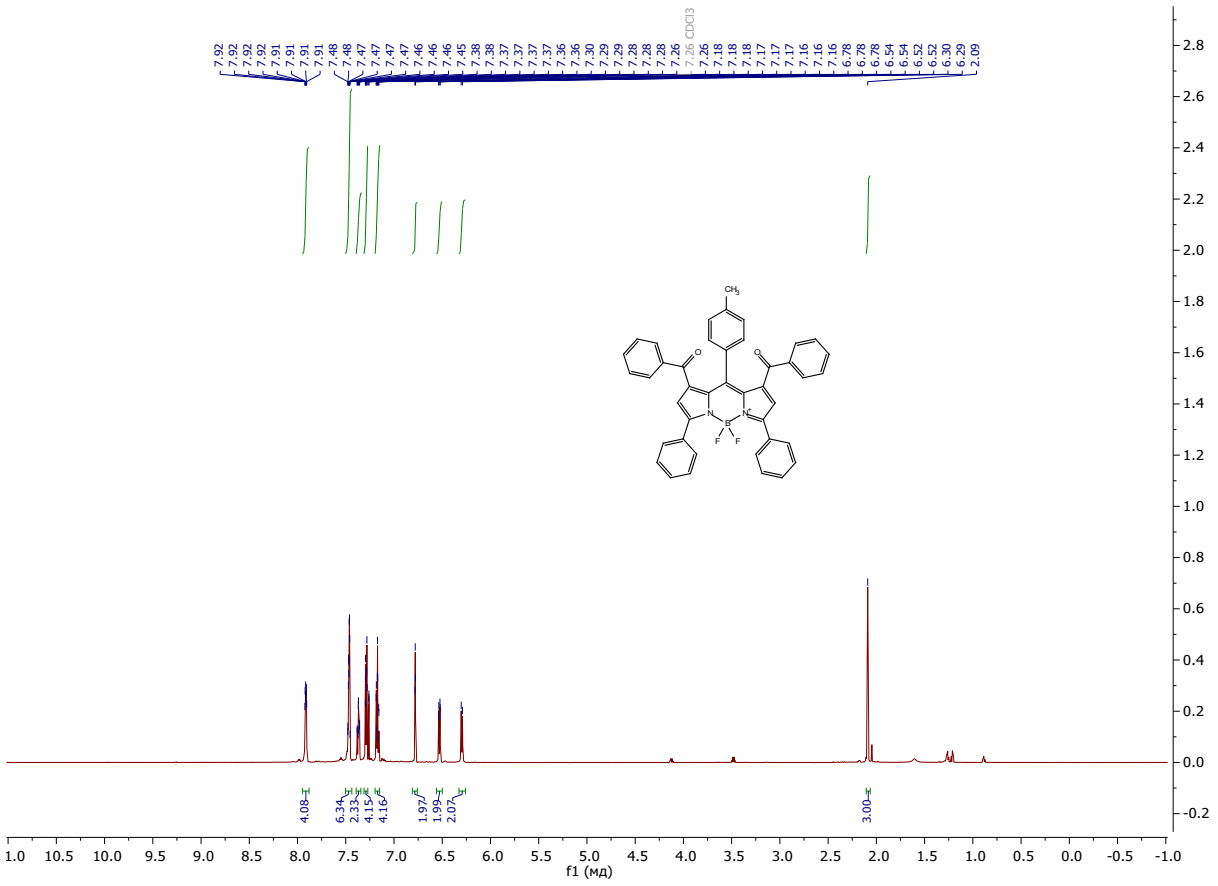

^{13}C NMR spectrum of **4f**

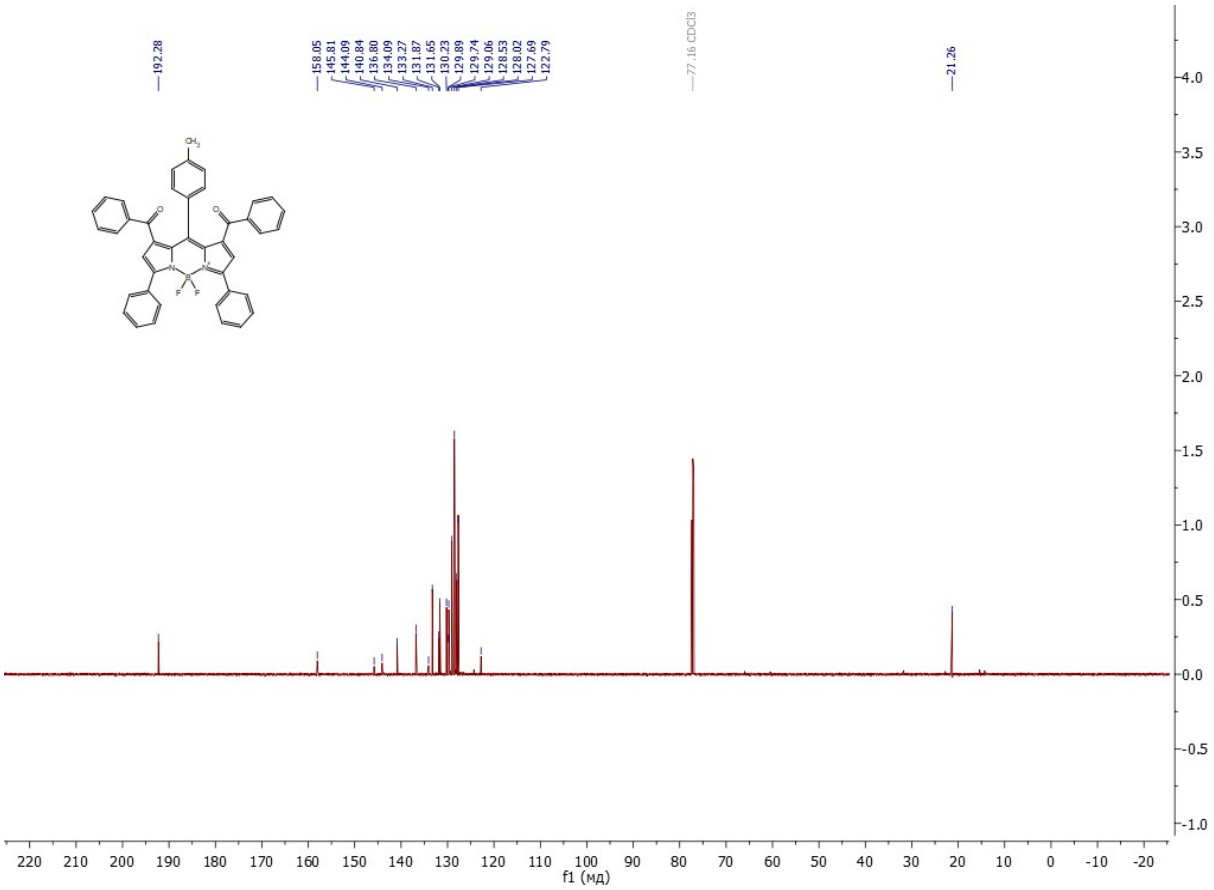

^{19}F NMR spectrum of **4f**

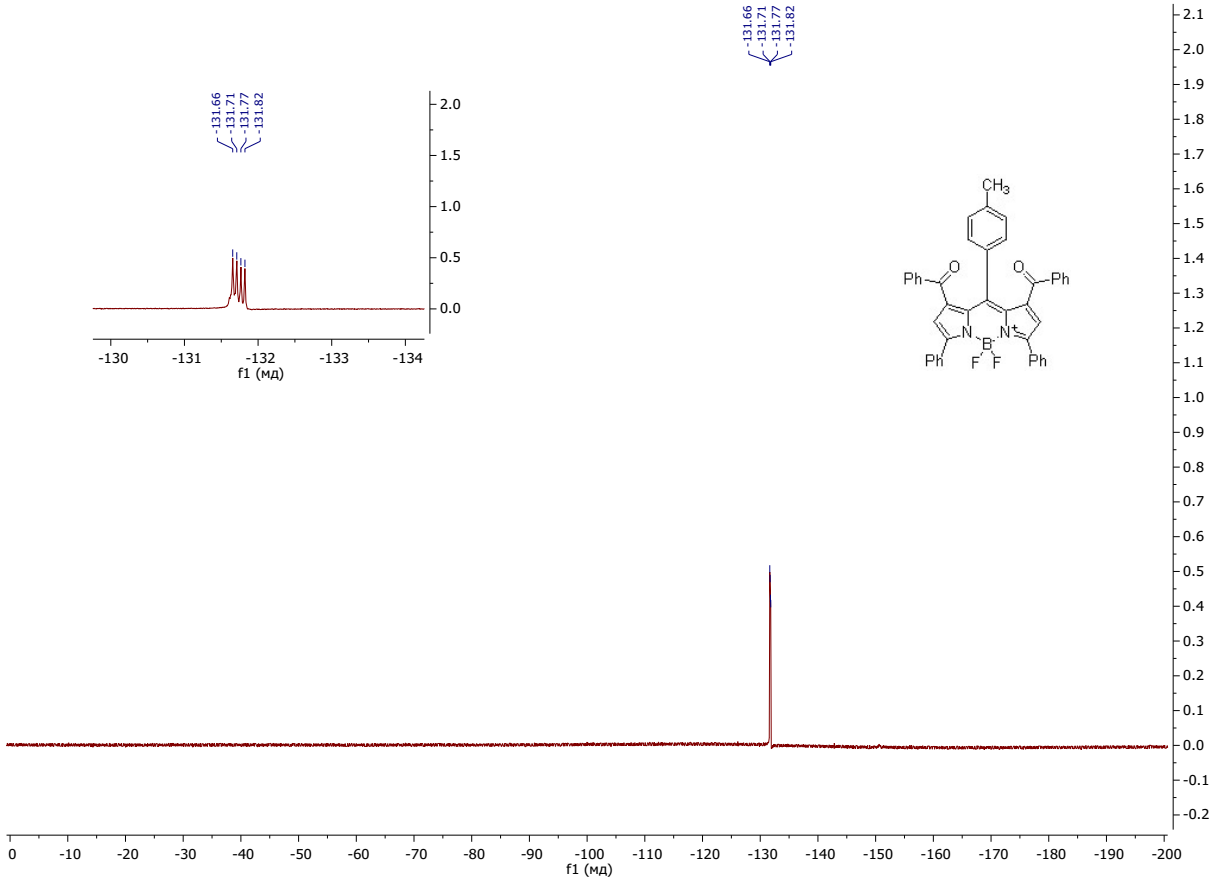

^{1}H NMR spectrum of **4g**

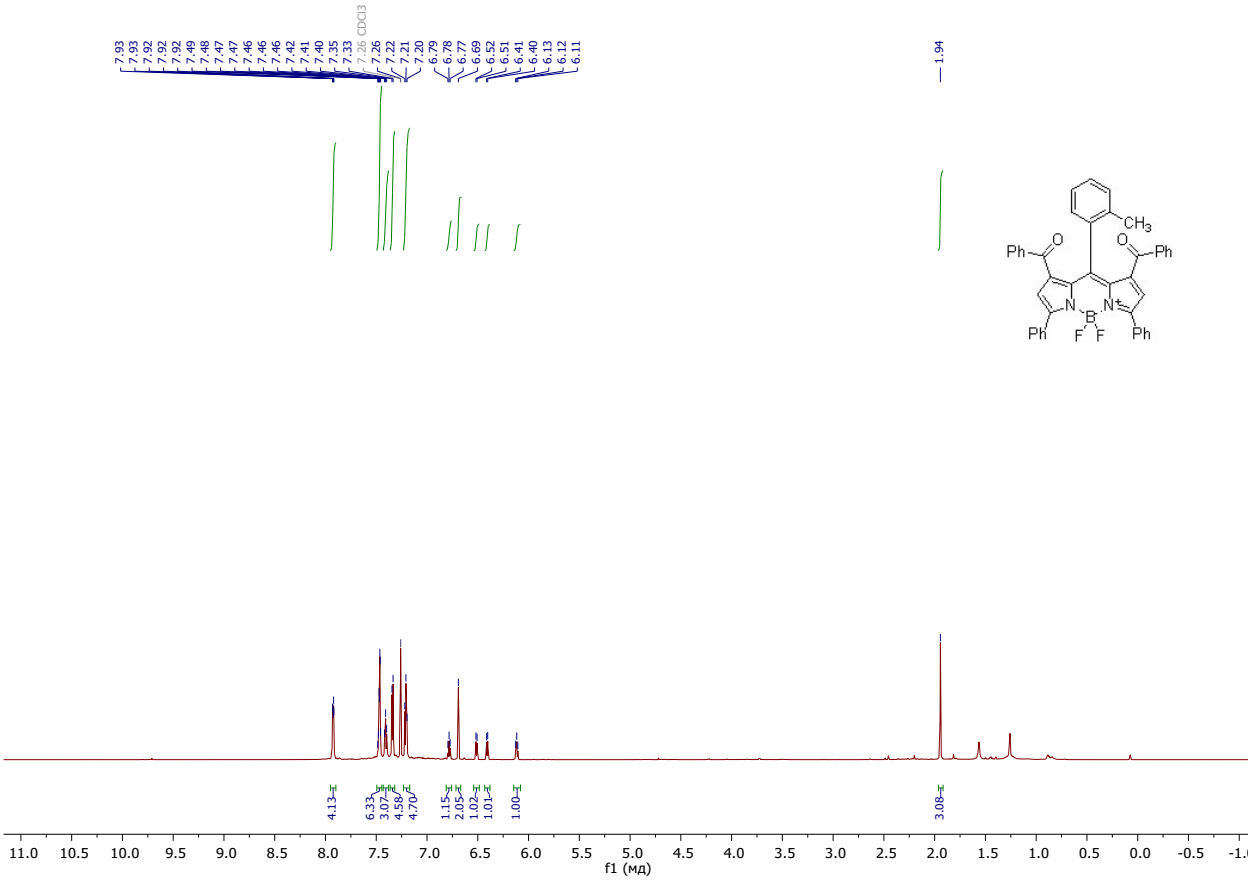

^{13}C NMR spectrum of **4g**

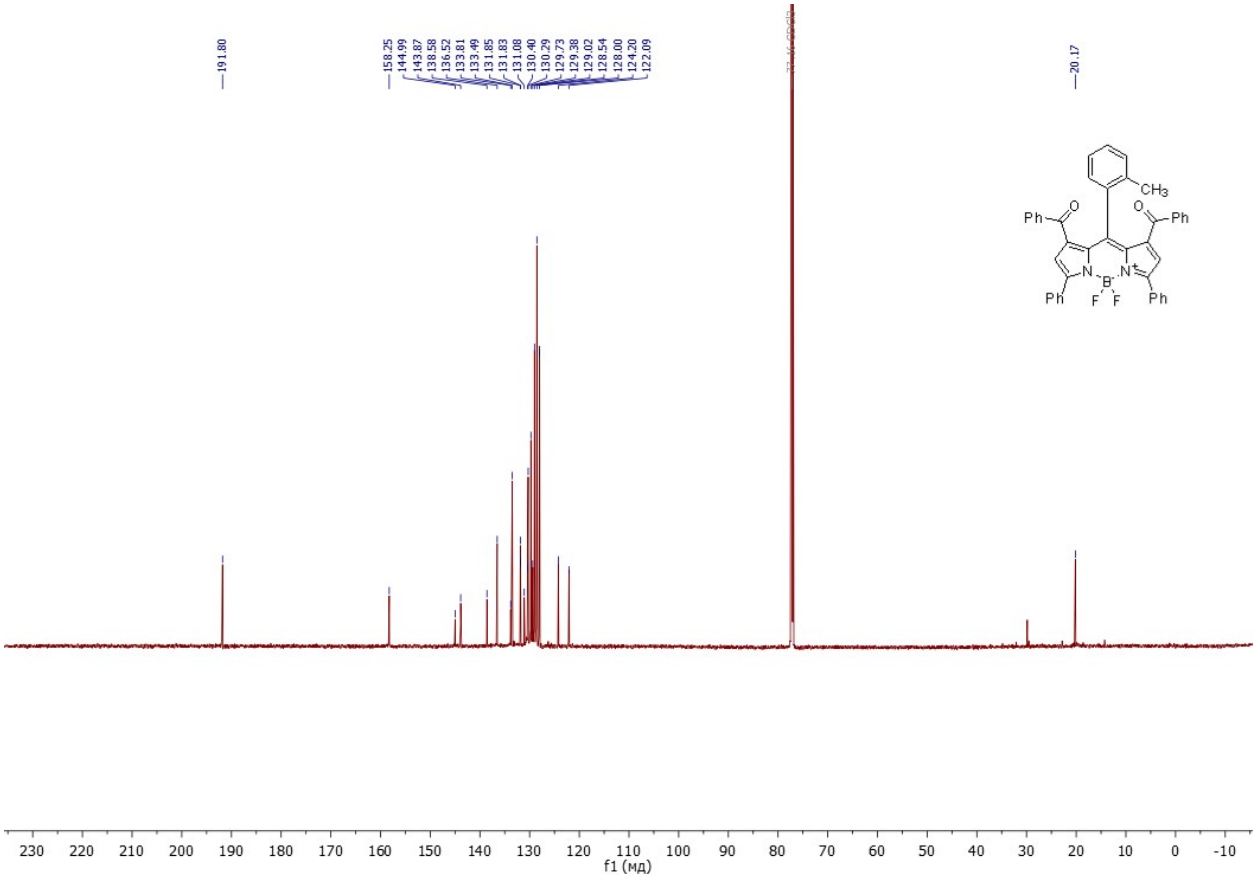

^{19}F NMR spectrum of **4g**

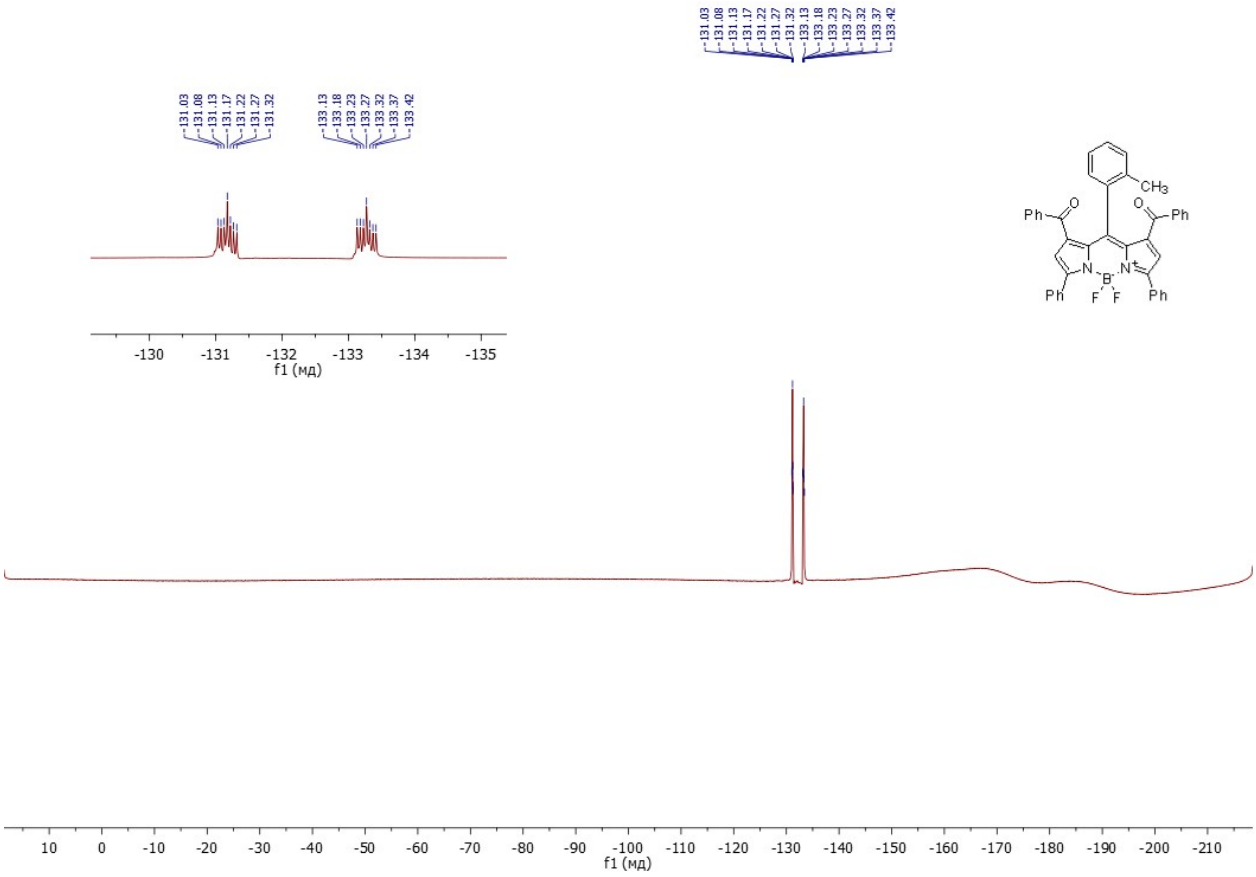

^{1}H NMR spectrum of **4h**

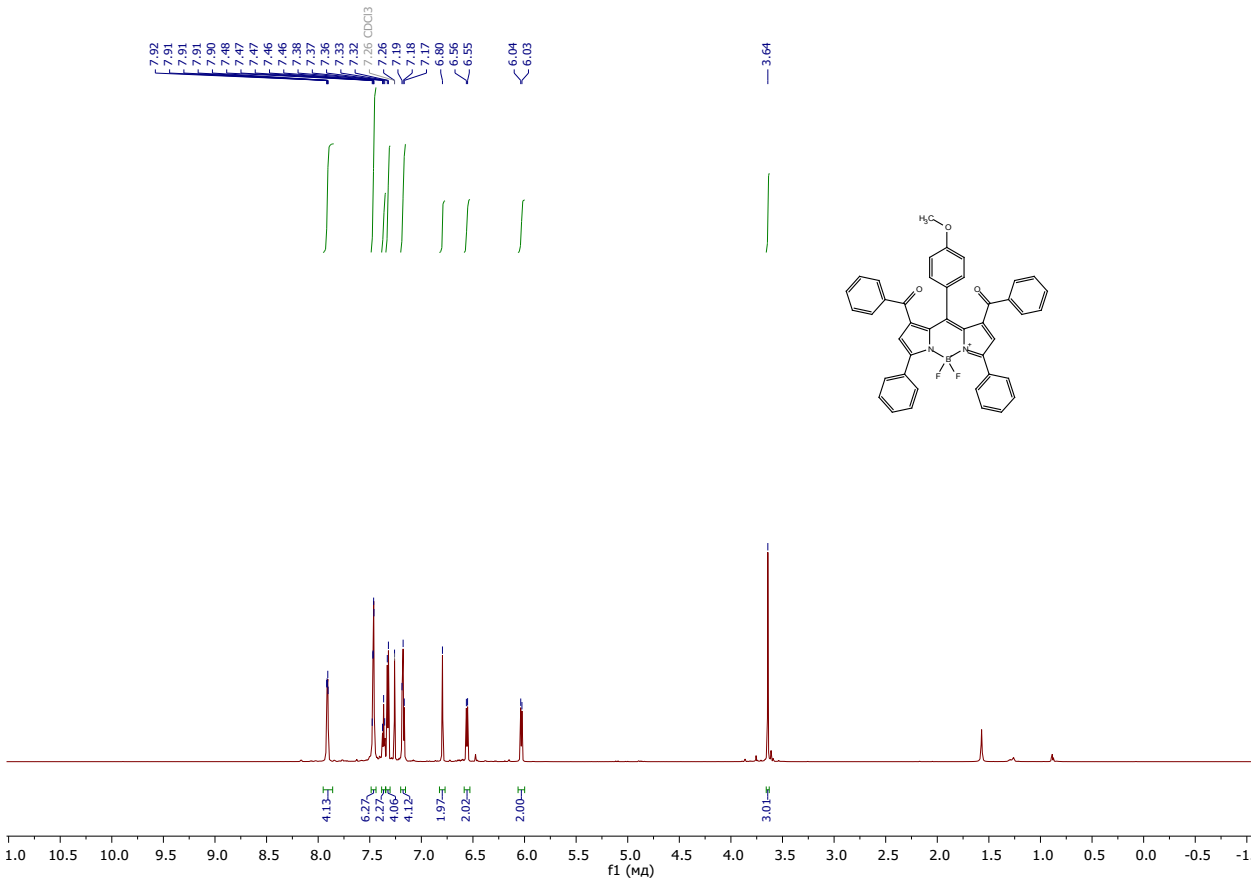

^{13}C NMR spectrum of **4h**

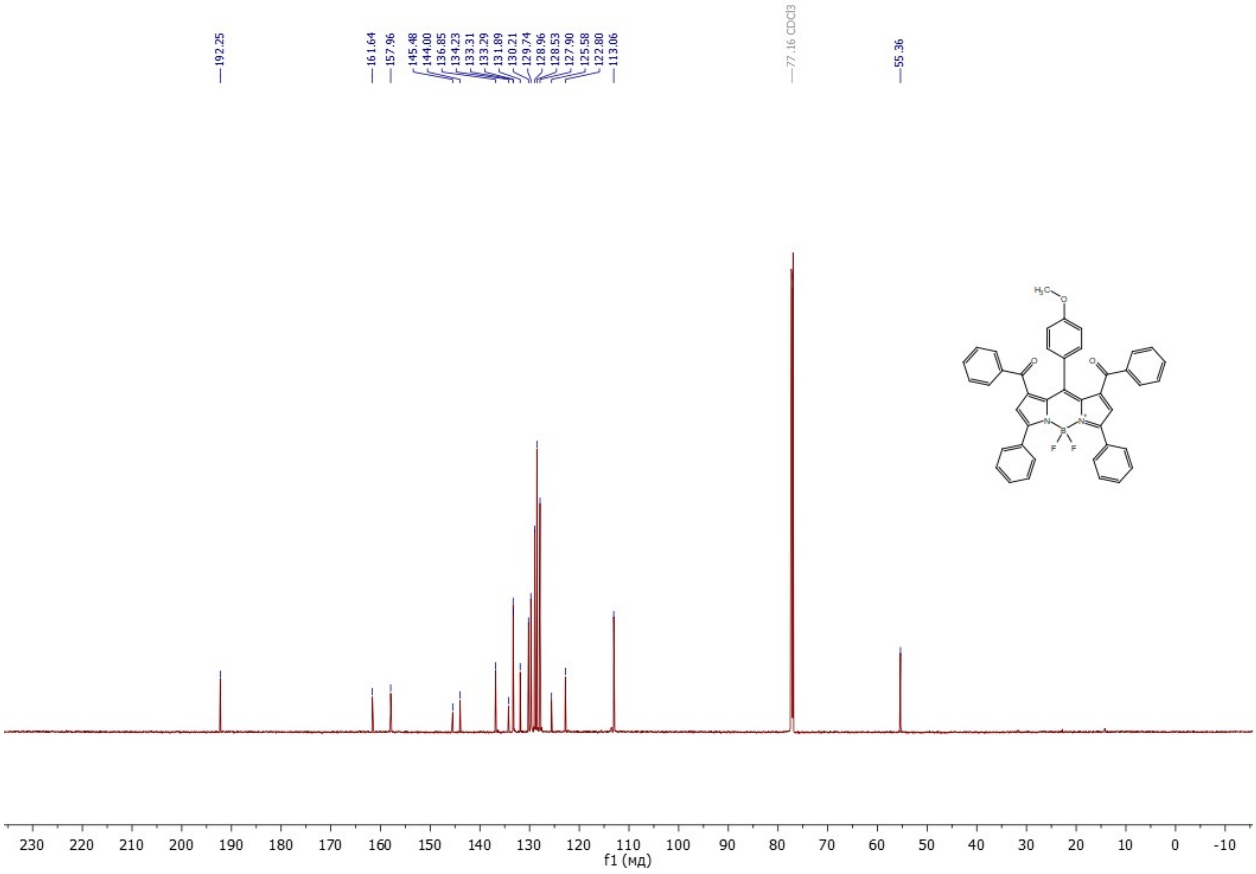

^{19}F NMR spectrum of **4h**

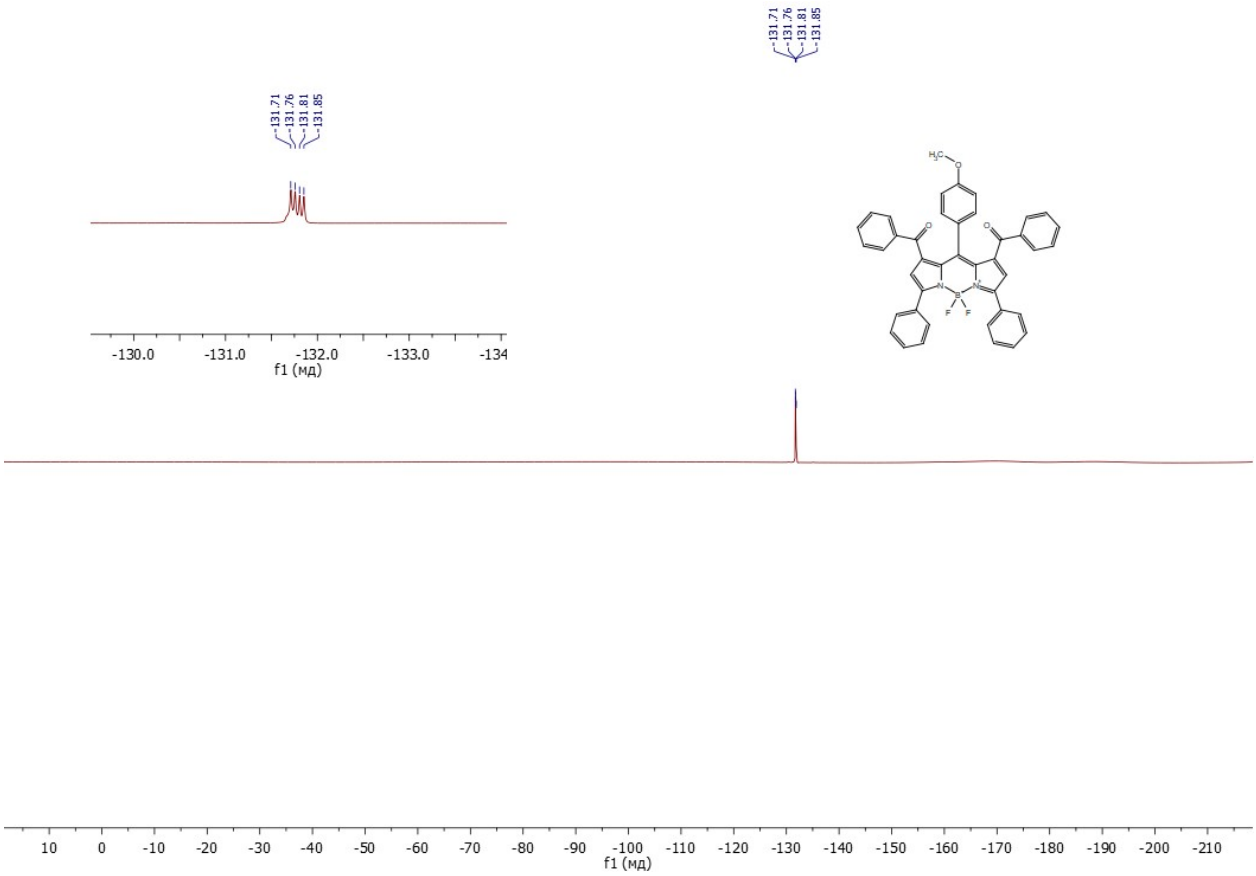
-131.71
-131.76
-131.81
-131.85
-130.0
-131.0
-132.0
-133.0
f1 (мд)
10
0
-10
-20
-30
-40
-50
-60
-70
-80
-90
-100
-110
-120
-130
-140
-150
-160
-170
-180
-190
-200
-210
f1 (мд)

^{1}H NMR spectrum of **4i**

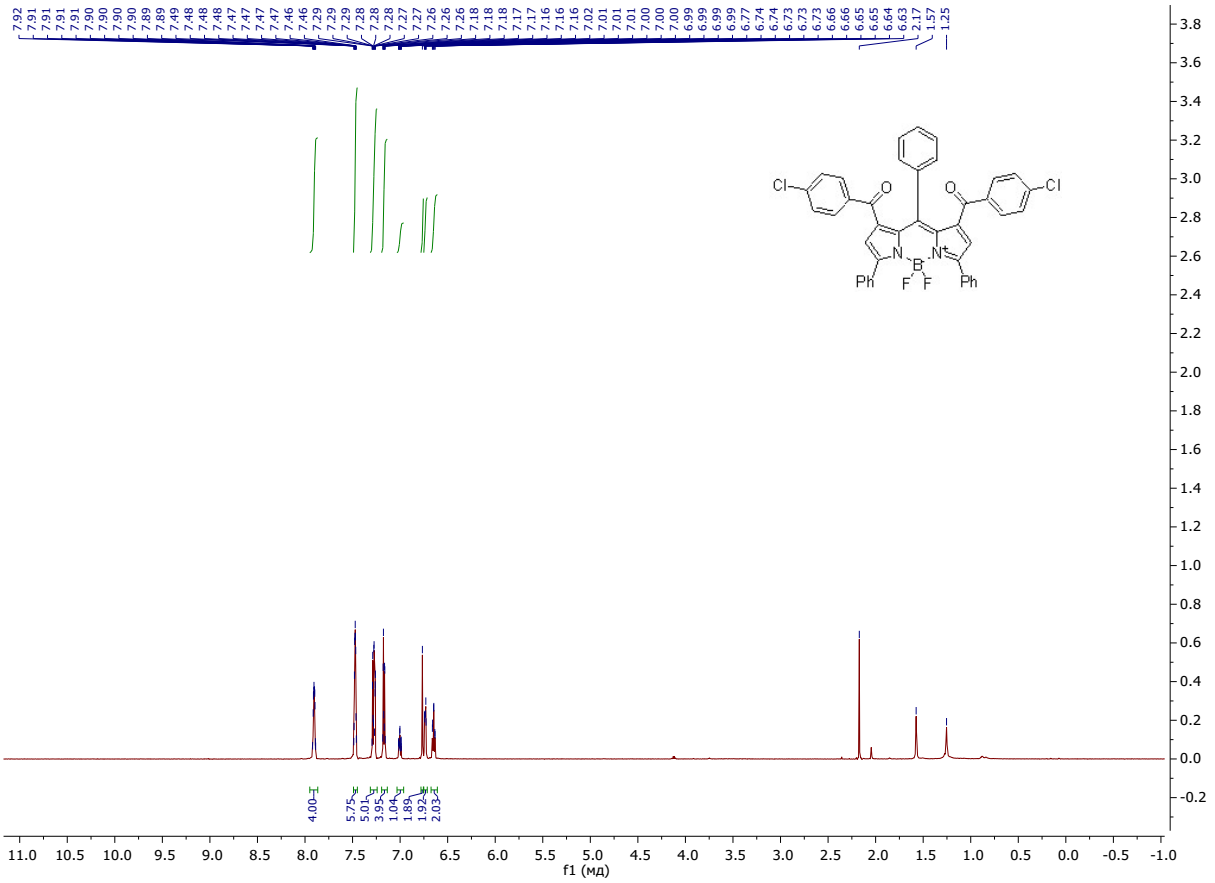

^{13}C NMR spectrum of **4i**

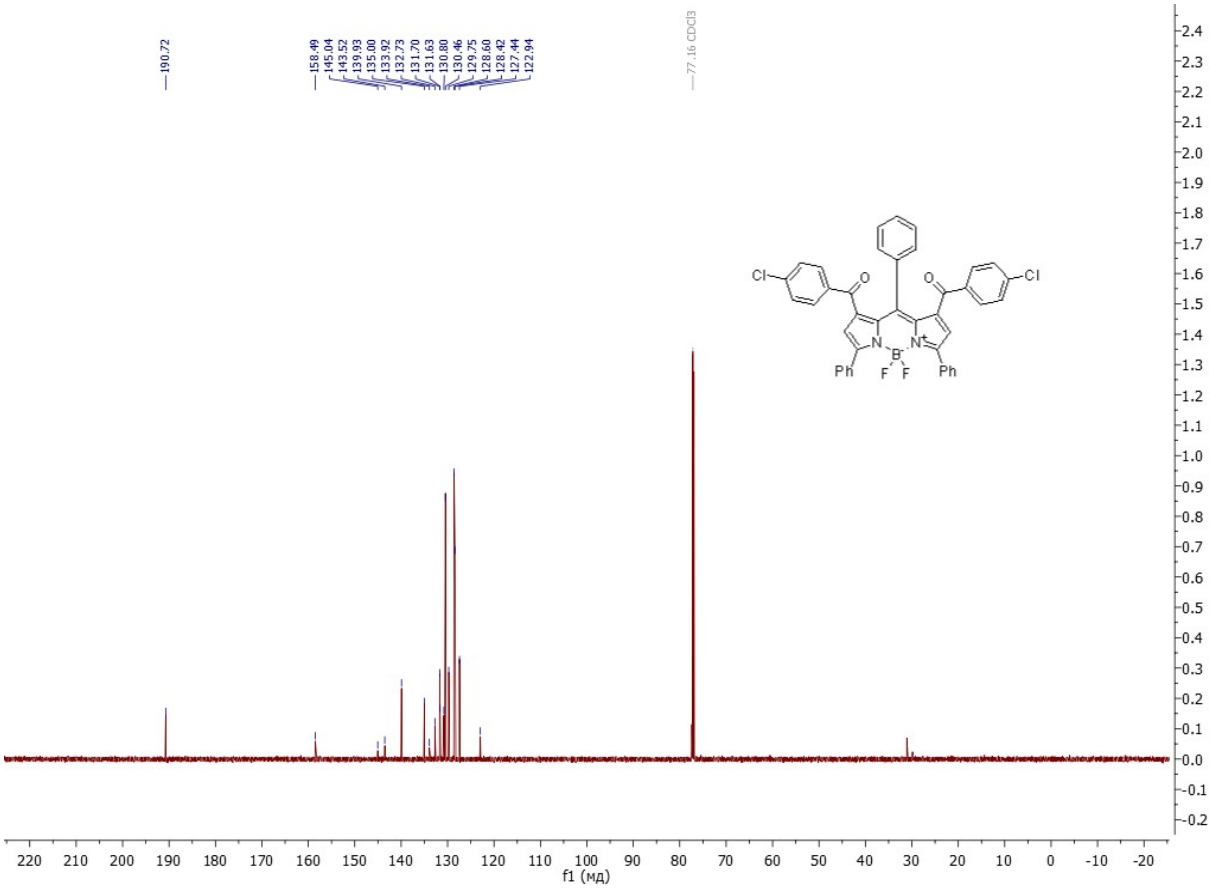

^{19}F NMR spectrum of **4i**

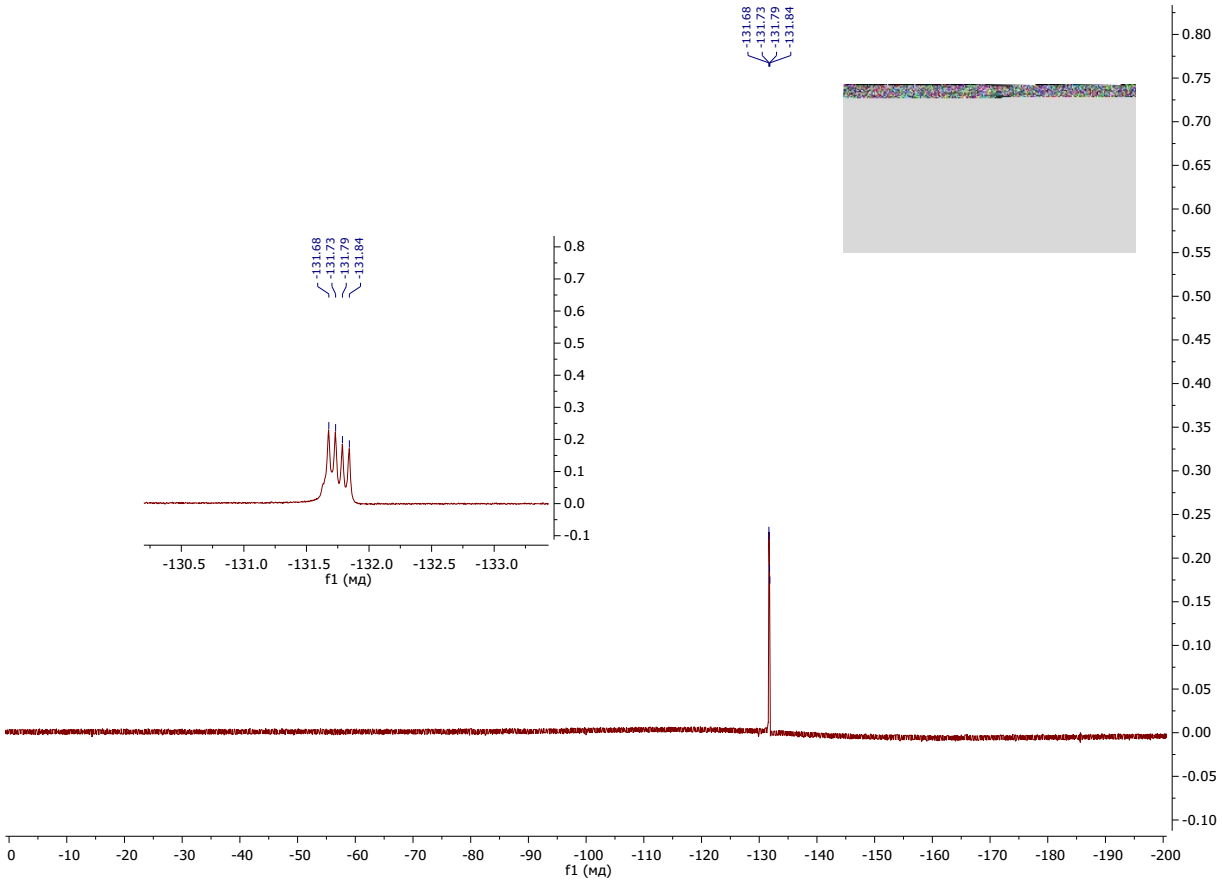

^{1}H NMR spectrum of **4j**

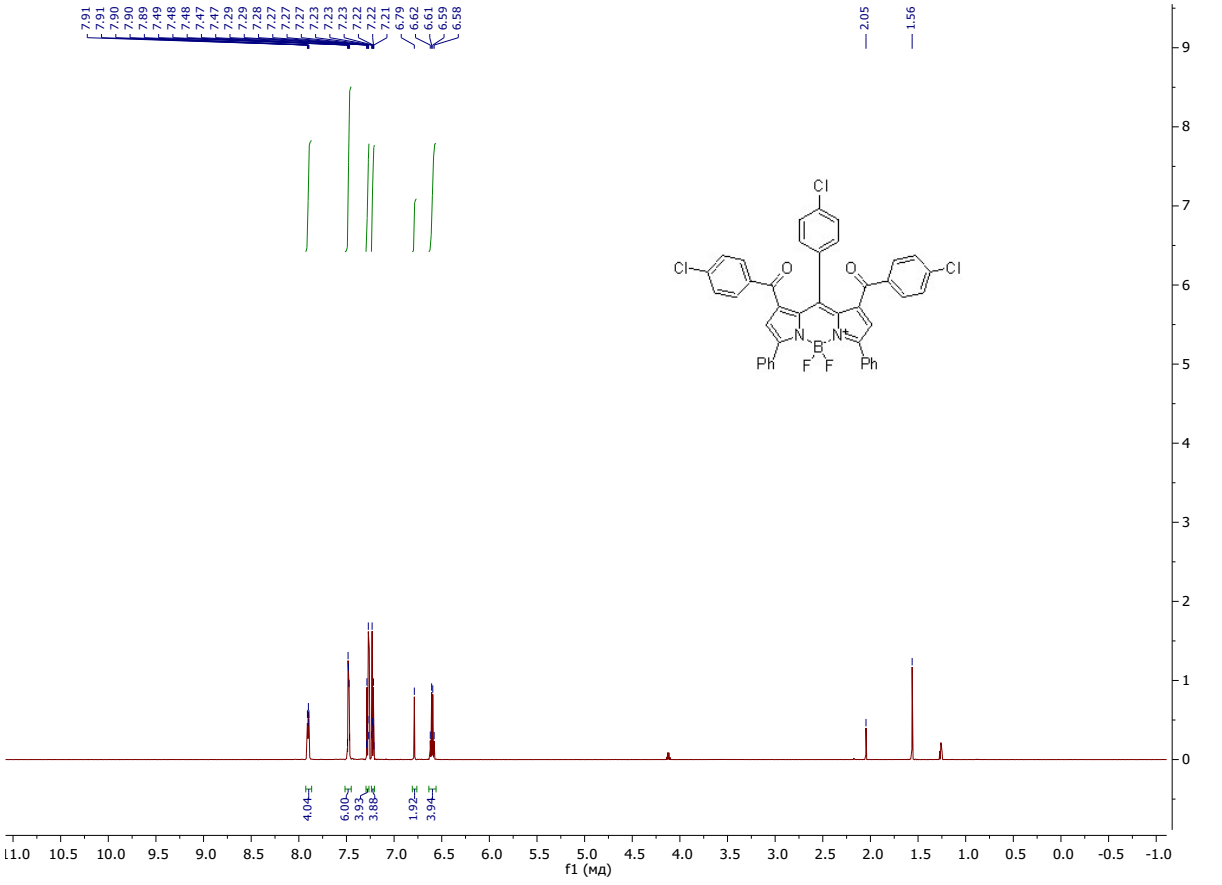

^{13}C NMR spectrum of **4j**

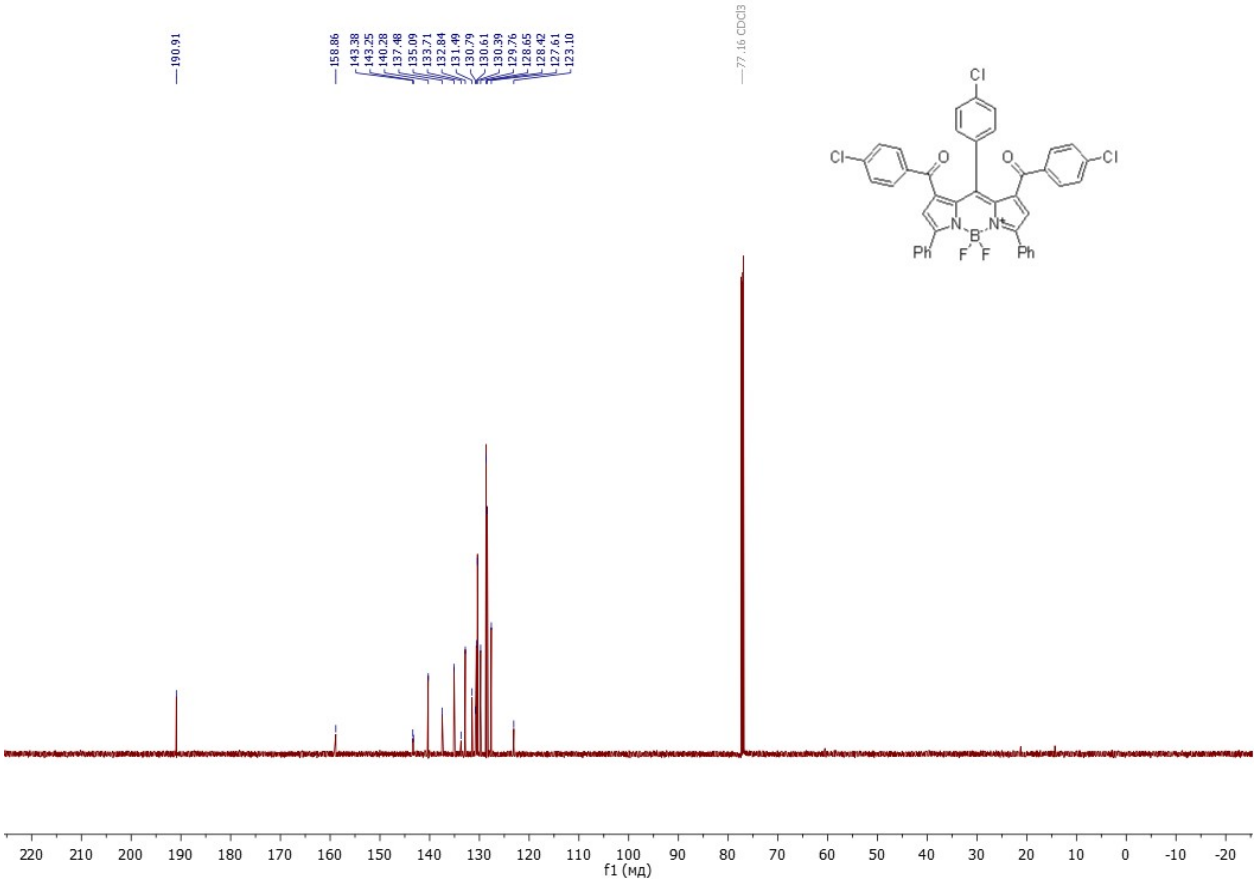

^{19}F NMR spectrum of **4j**

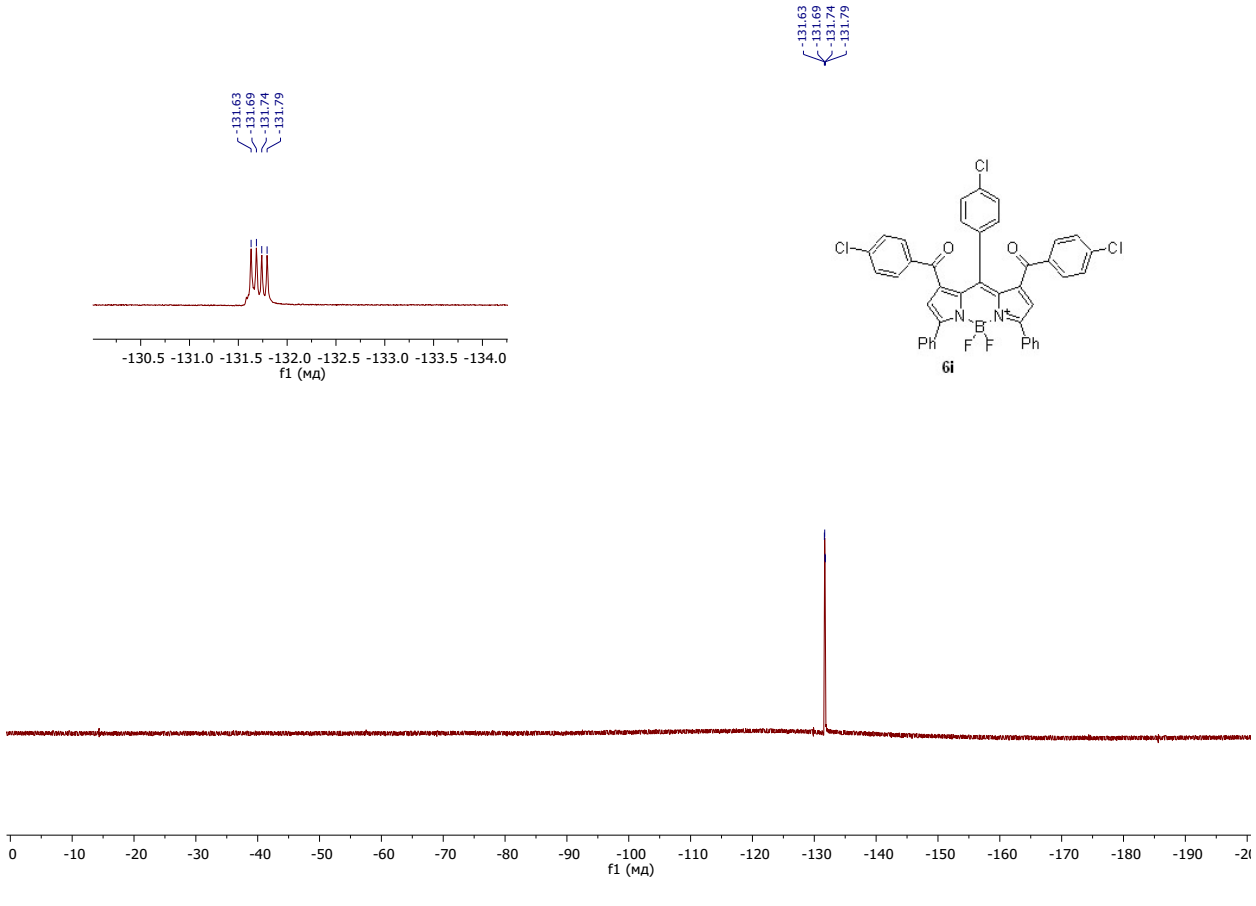

^{1}H NMR spectrum of **4k**

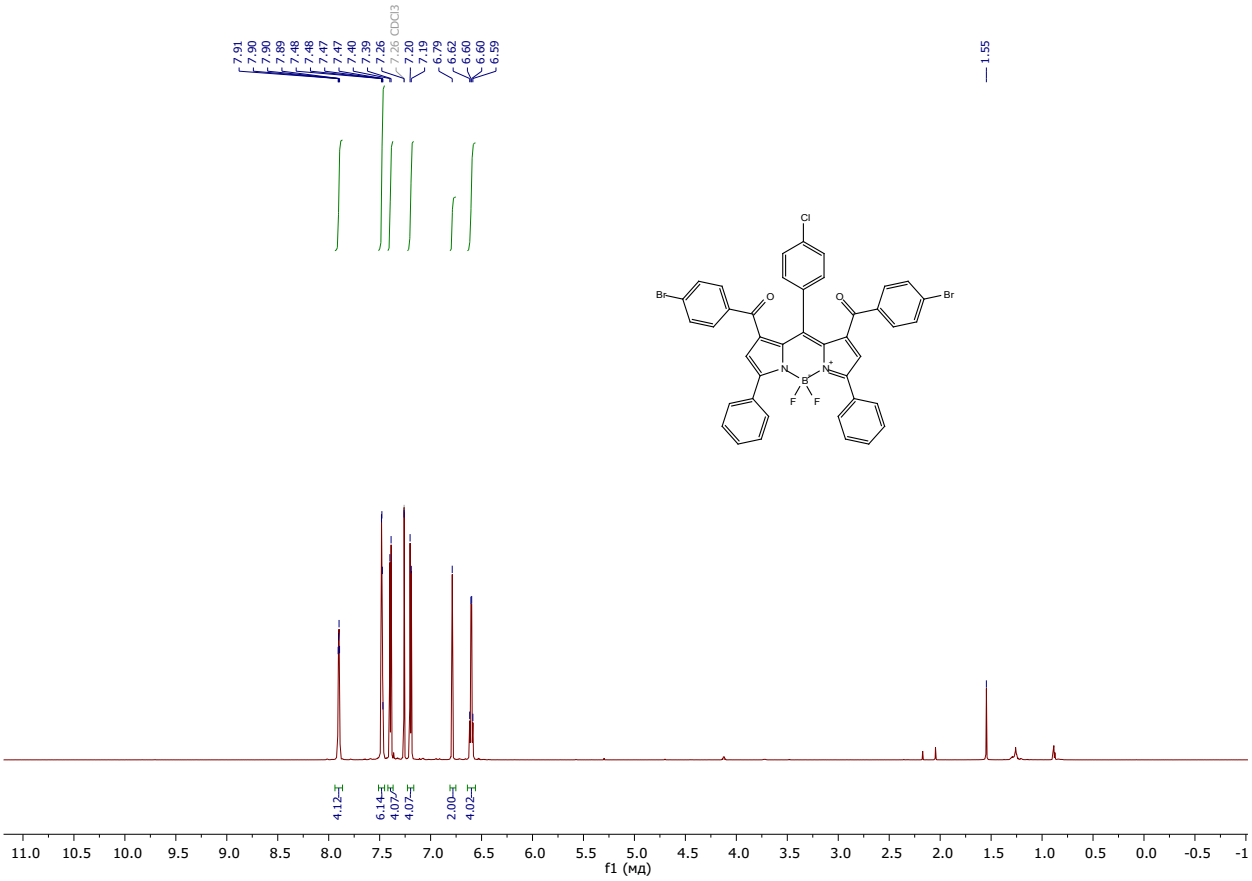

^{13}C NMR spectrum of **4k**

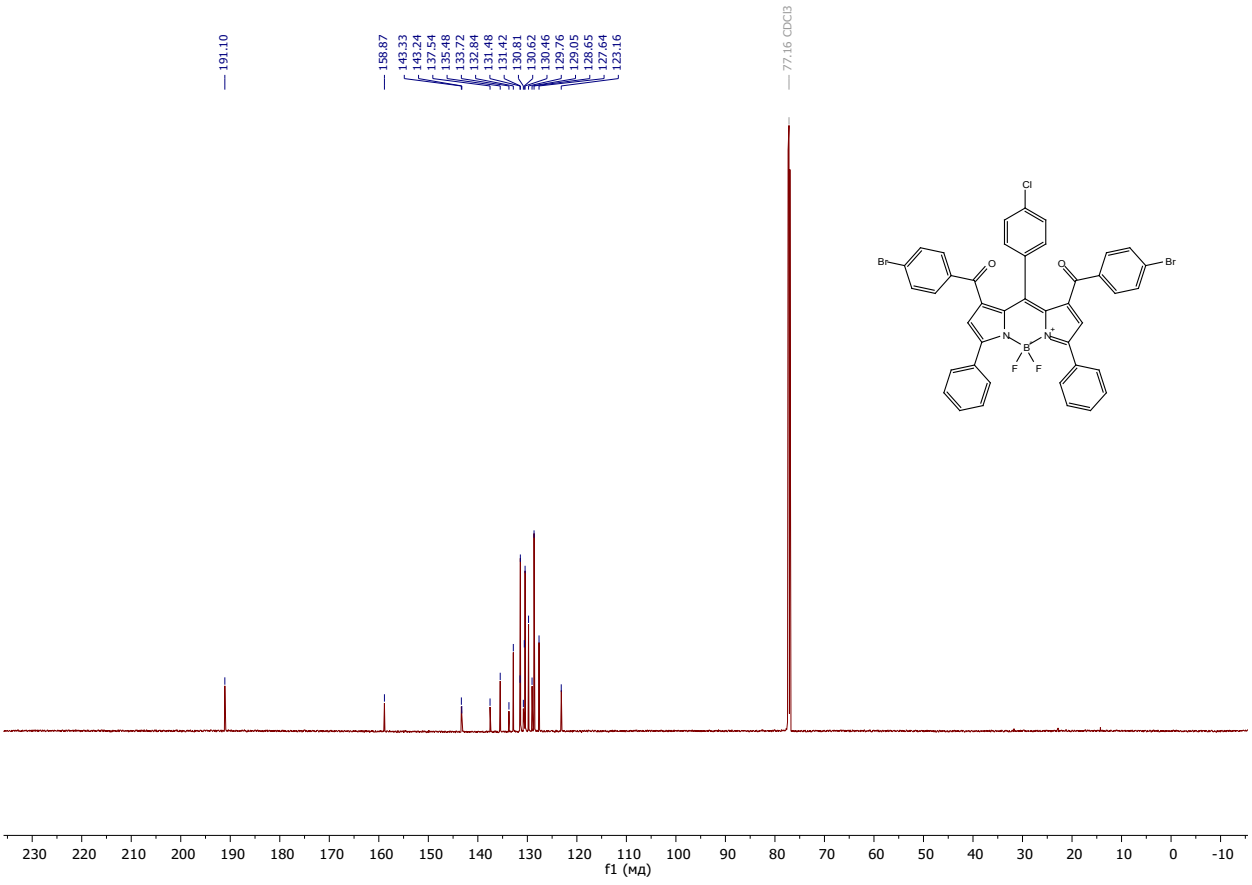

^{19}F NMR spectrum of **4k**

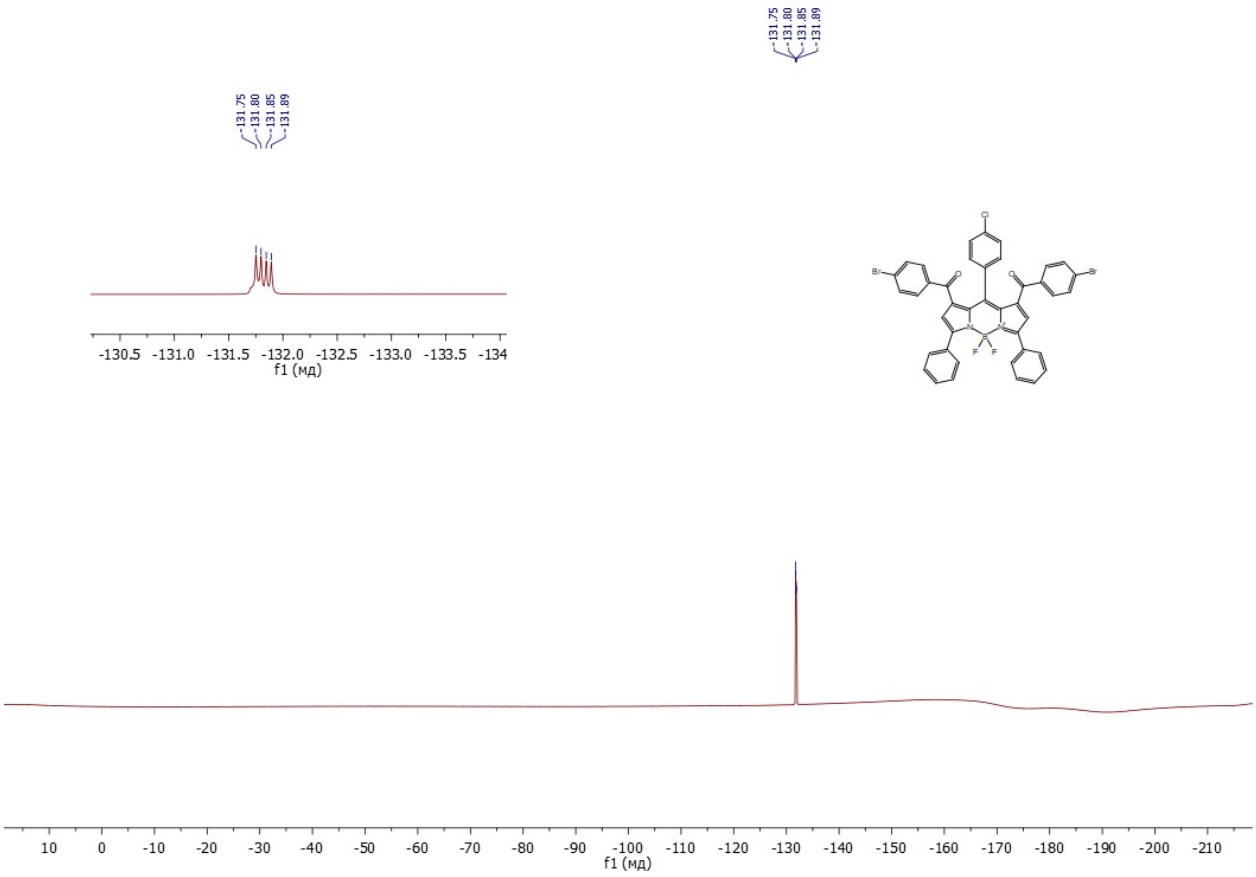

^{1}H NMR spectrum of **4l**

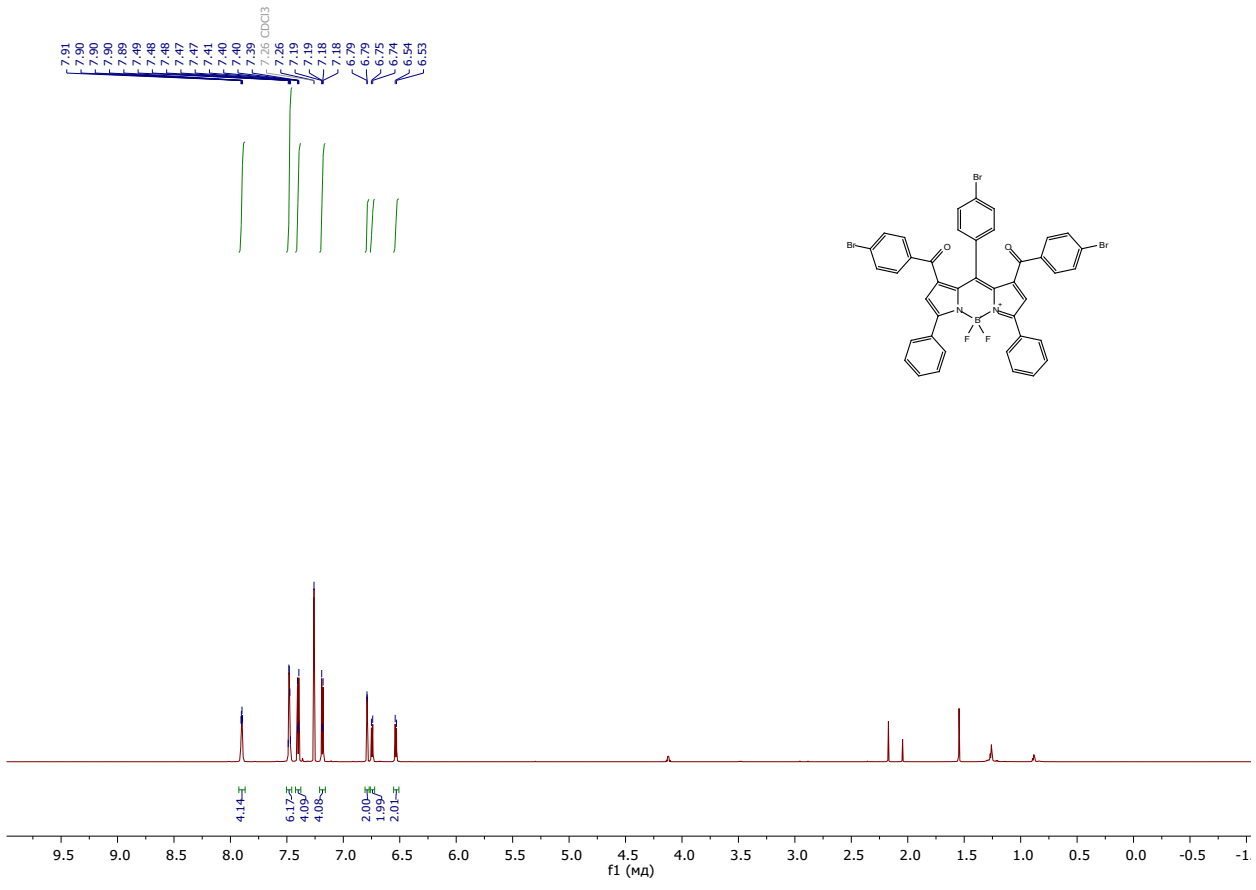

^{13}C NMR spectrum of **4l**

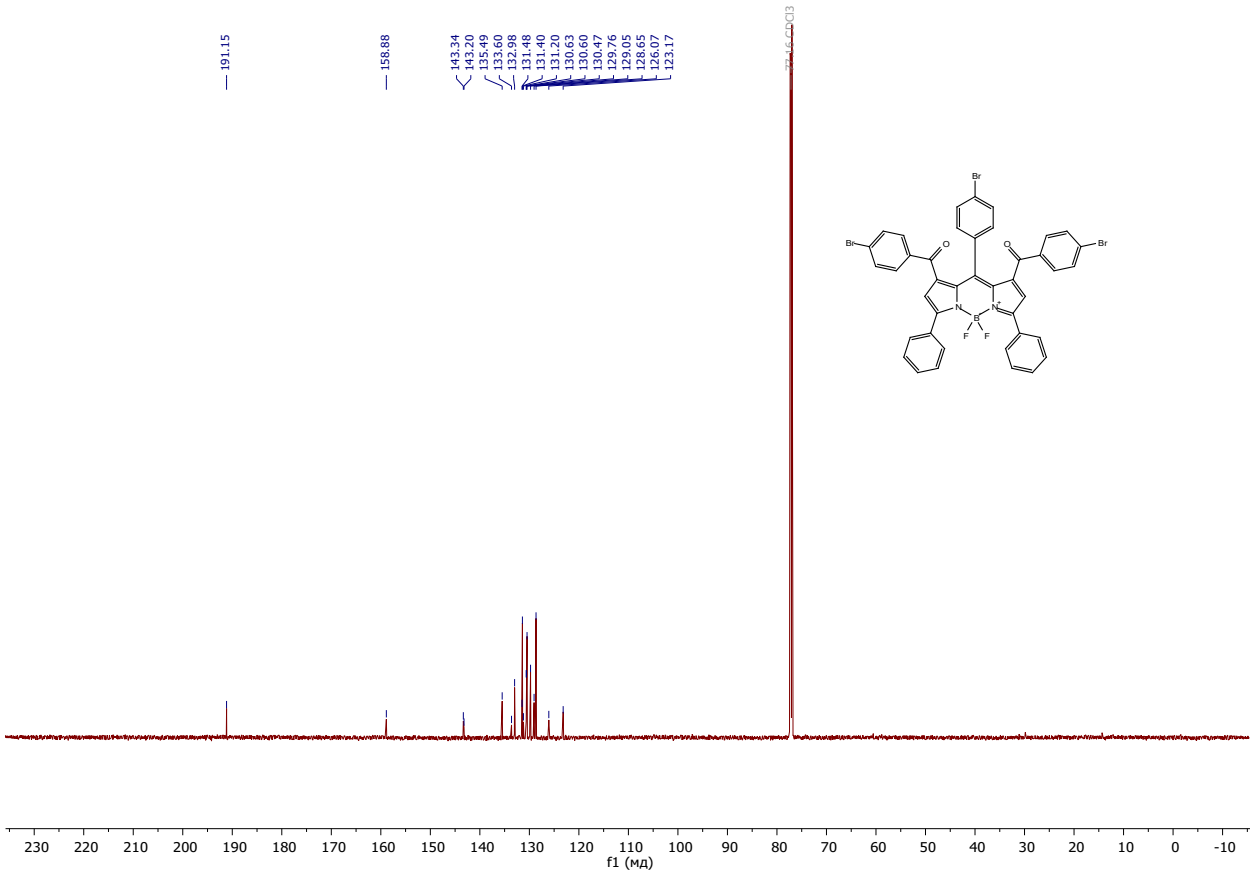

^{19}F NMR spectrum of **4l**

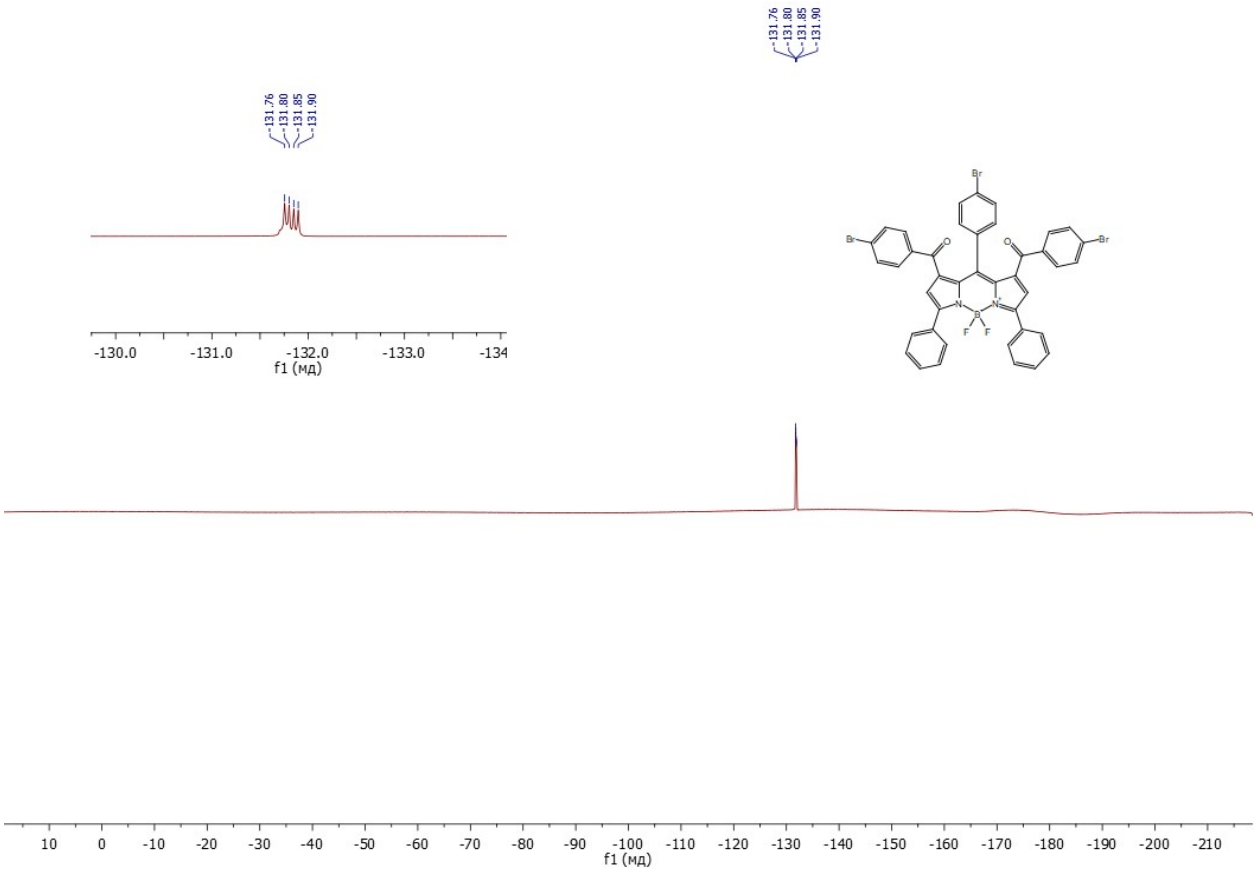

^{1}H NMR spectrum of **4m**

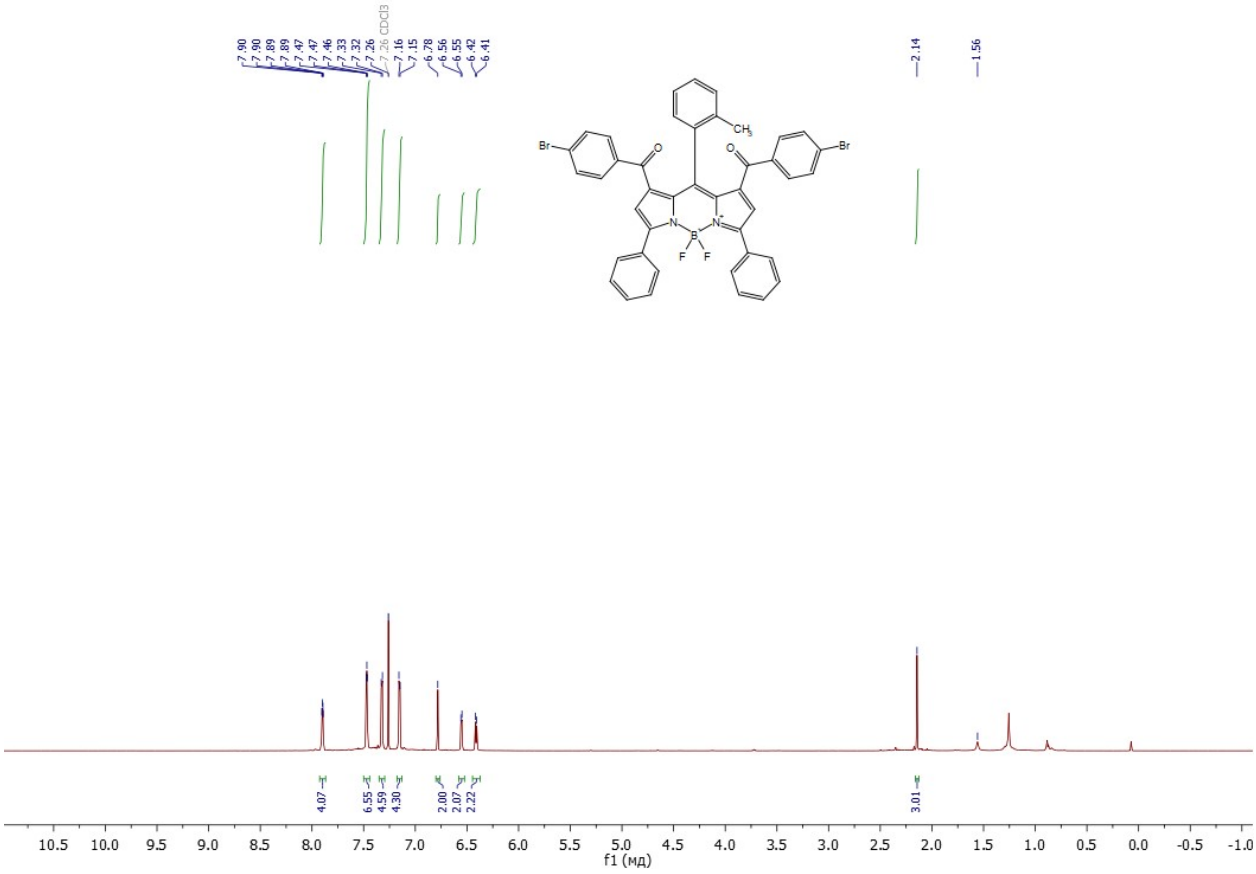

^{13}C NMR spectrum of **4m**

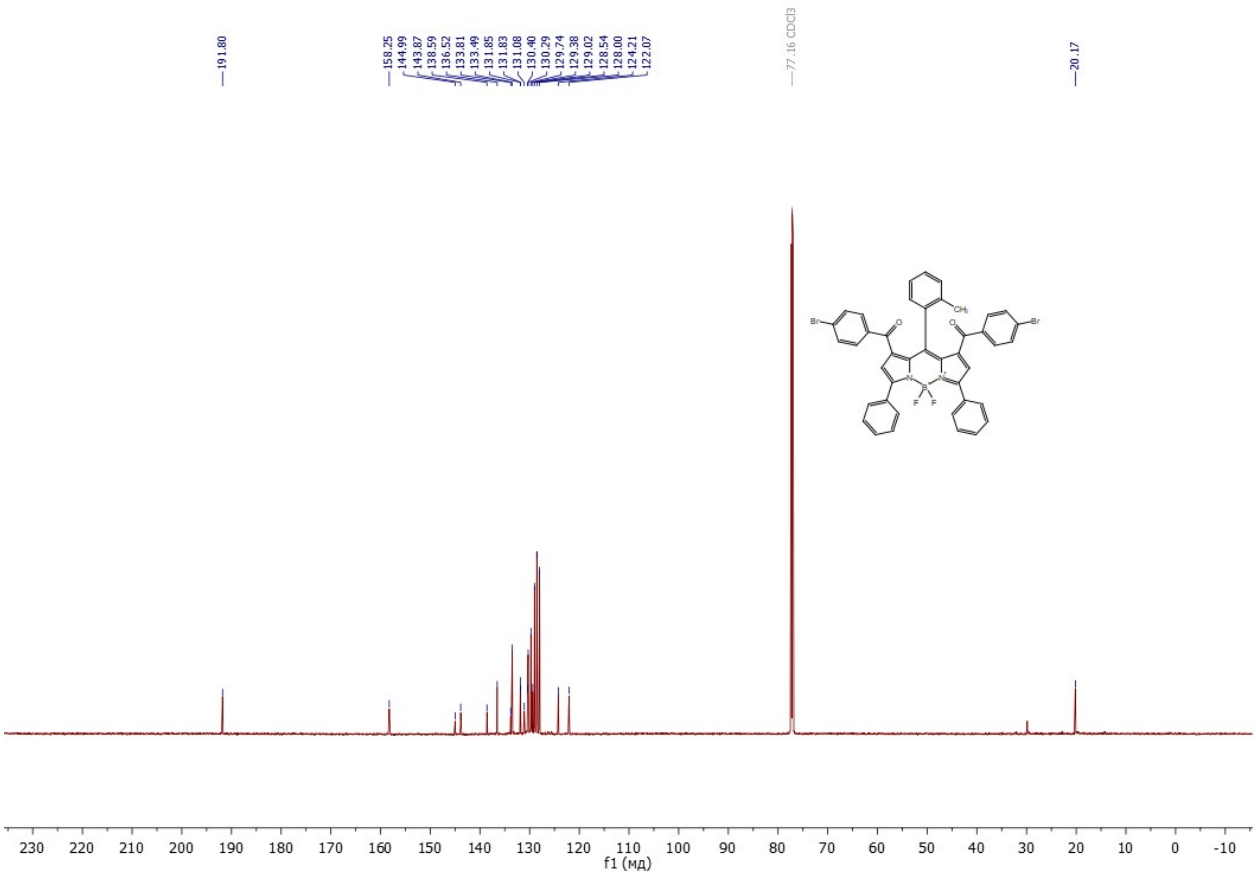
191.80
158.25
144.99
143.87
138.59
136.52
133.81
133.49
131.85
131.83
131.08
130.40
130.29
129.74
129.38
129.02
128.54
128.00
124.21
122.07
77.16 CDCl3
20.17
Br
O
O
Br
CH3
N
N
B
F
F
230 220 210 200 190 180 170 160 150 140 130 120 110 100 90 80 70 60 50 40 30 20 10 0 -10
f1 (мд)

^{19}F NMR spectrum of **4m**

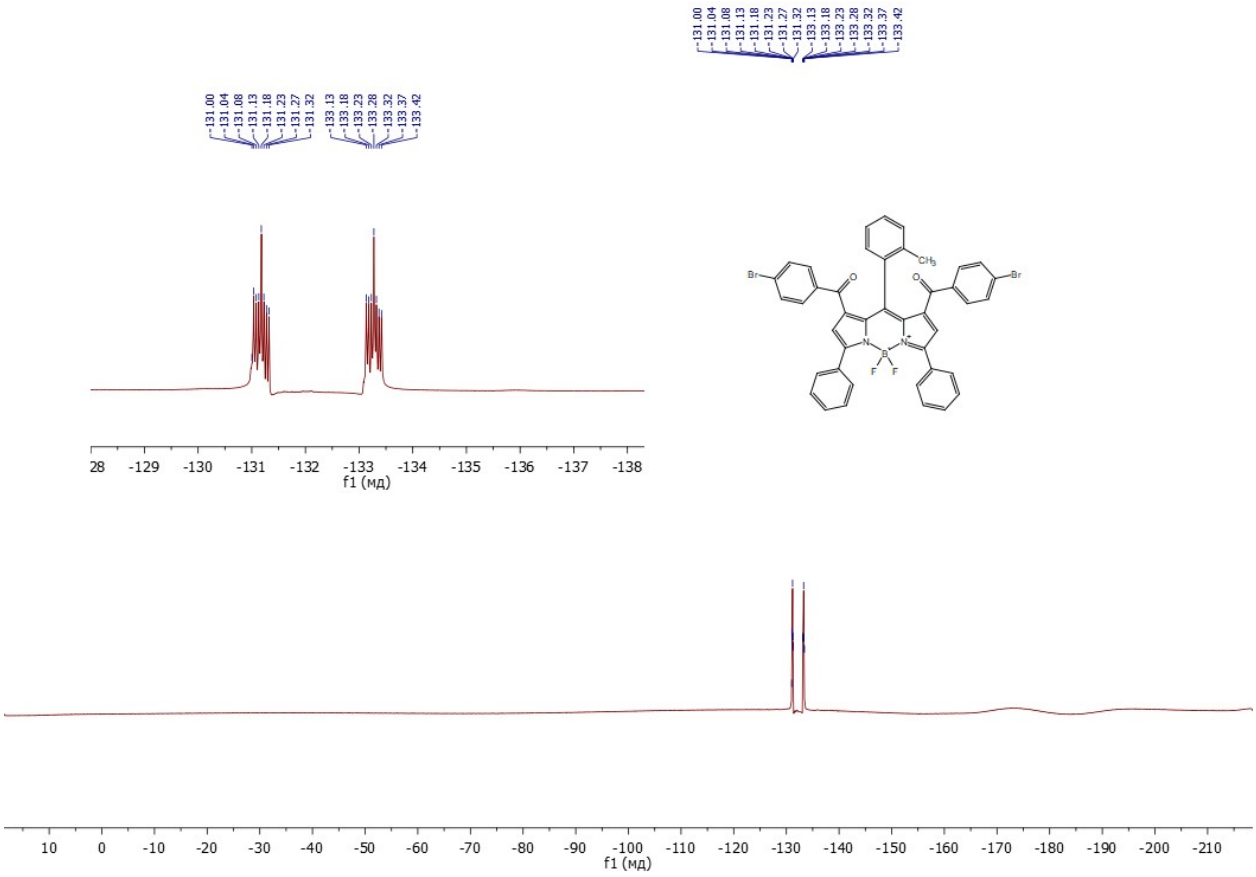

^{1}H NMR spectrum of **4n**

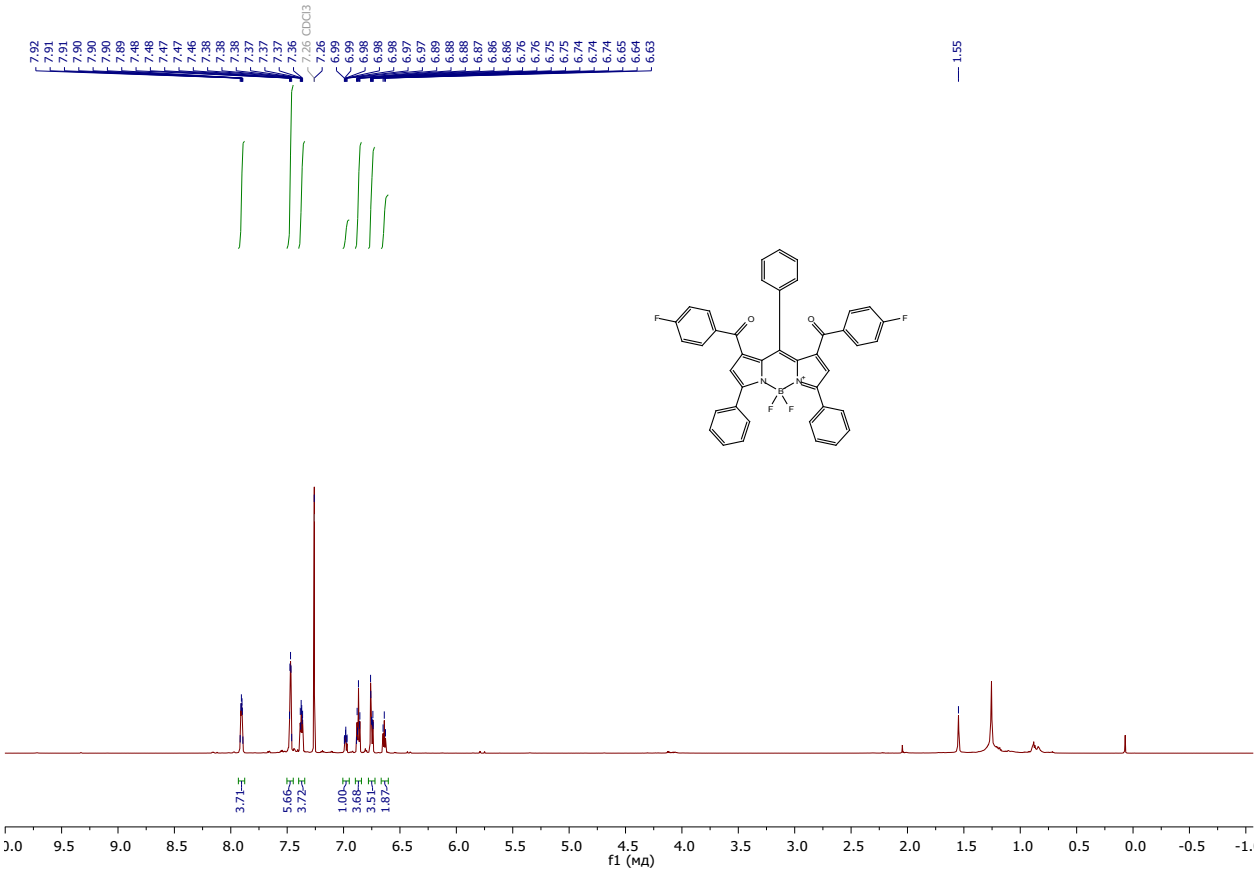
7.92
7.91
7.91
7.90
7.90
7.90
7.89
7.48
7.48
7.47
7.47
7.46
7.38
7.38
7.38
7.37
7.37
7.37
7.36
7.26 CDCl3
7.26
6.99
6.99
6.98
6.98
6.98
6.97
6.89
6.88
6.87
6.86
6.76
6.76
6.75
6.74
6.74
6.74
6.65
6.64
6.63
1.55
F
O
O
F
N
B
N+
F
F
3.71
5.66
3.72
1.00
3.68
3.51
1.87
f1 (мд)

^{13}C NMR spectrum of **4n**

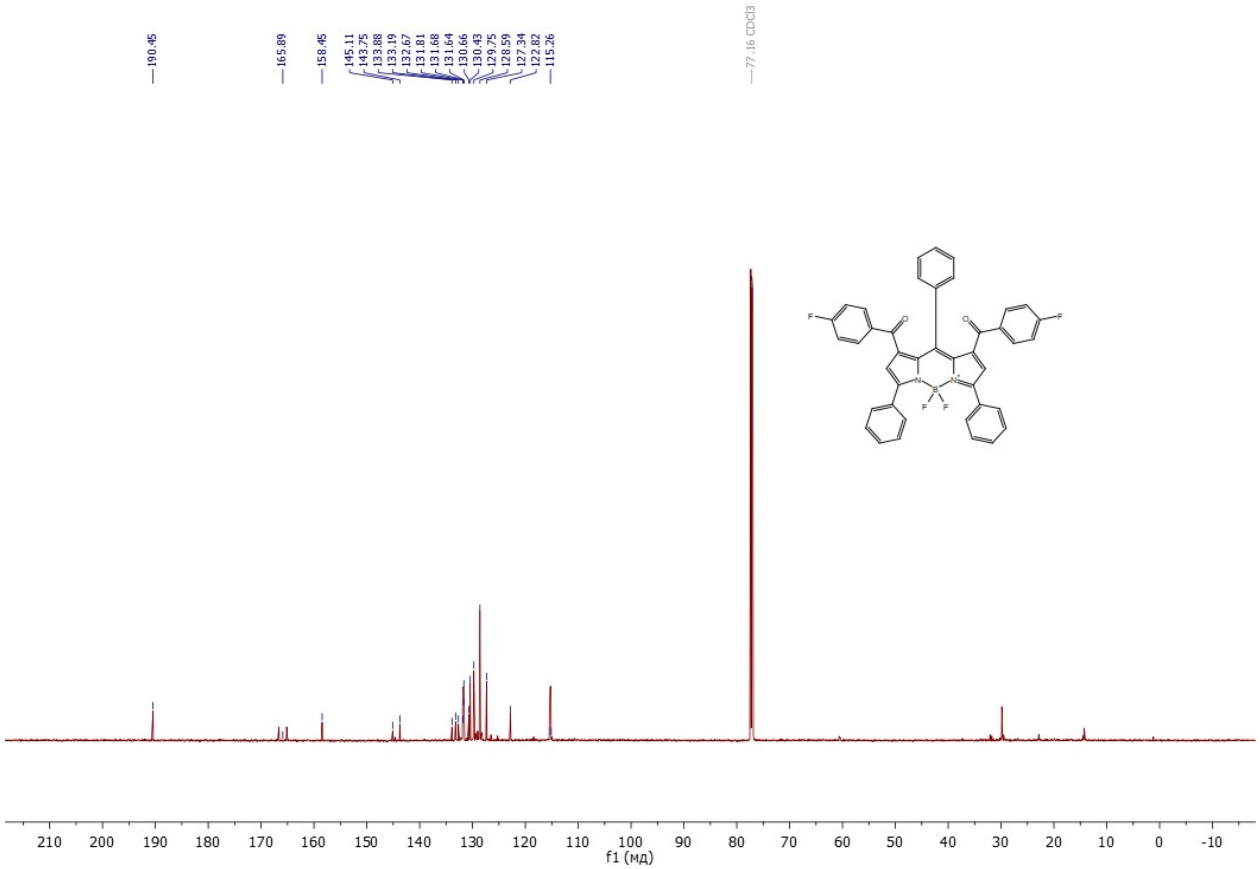

^{19}F NMR spectrum of **4n**

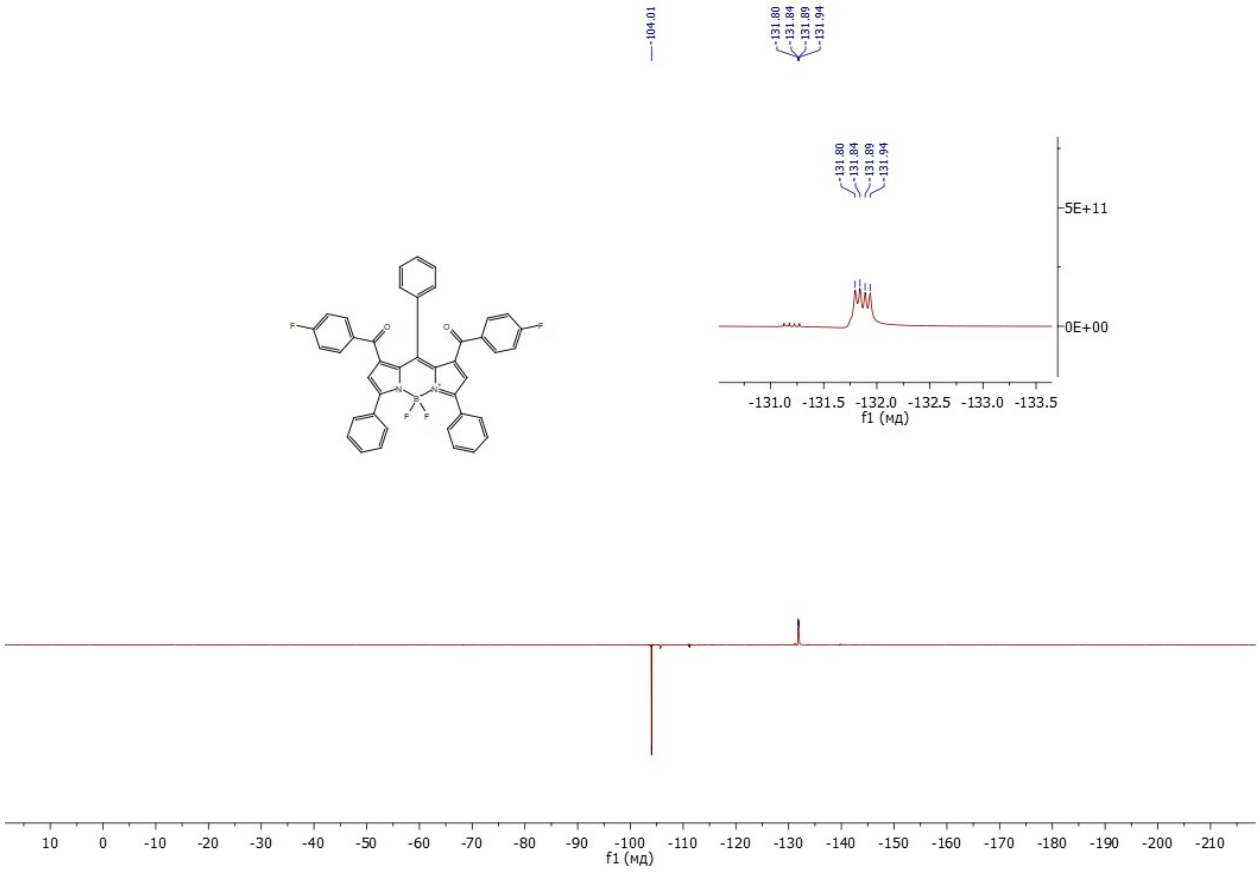

2. HRMS

4a

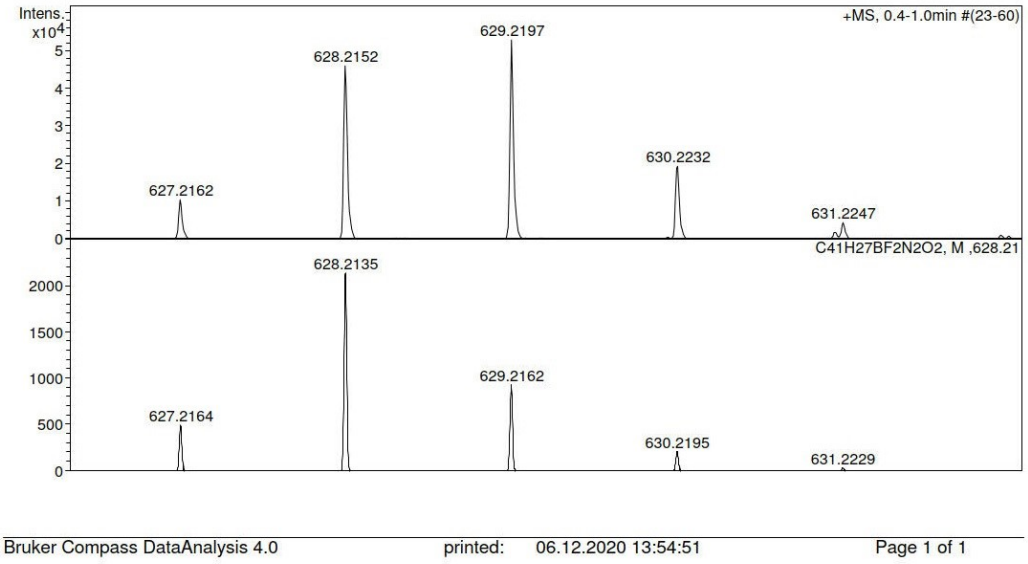

Bruker Compass DataAnalysis 4.0 printed: 06.12.2020 13:54:51 Page 1 of 1

4b

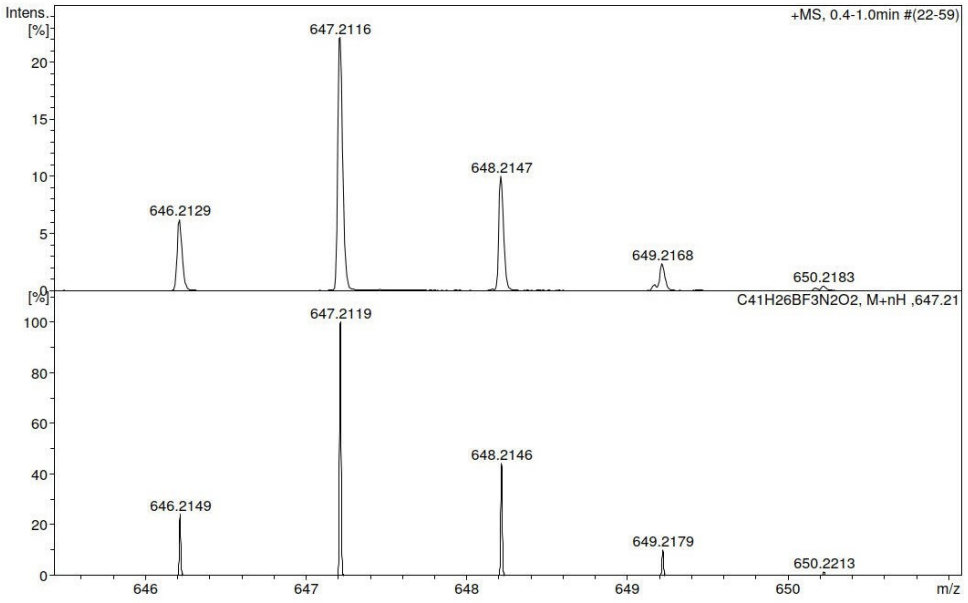

Bruker Compass DataAnalysis 4.0 printed: 03.05.2021 17:28:06 Page 1 of 1

4c

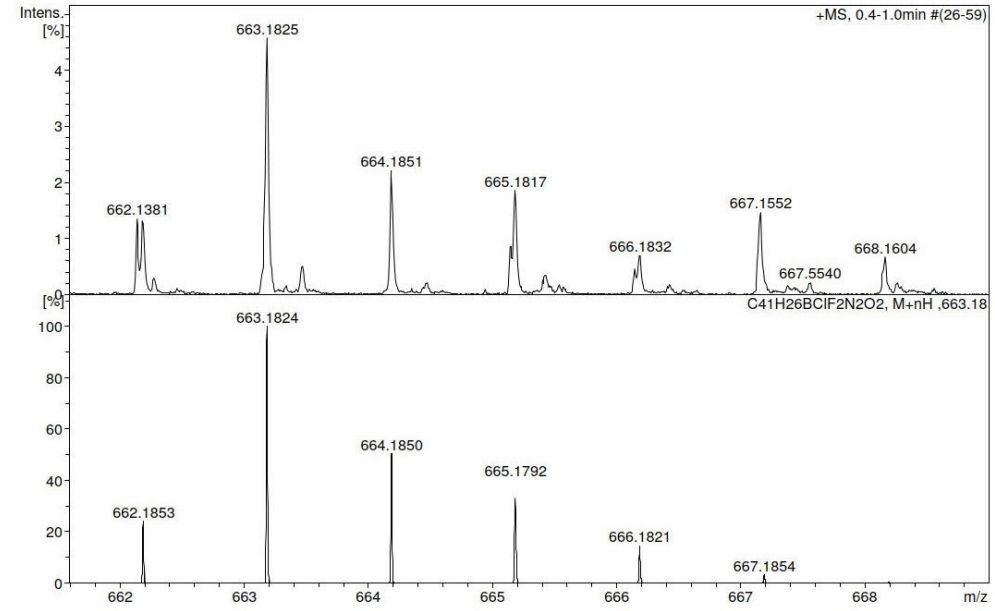

Bruker Compass DataAnalysis 4.0 printed: 03.05.2021 17:29:53 Page 1 of 1

4d

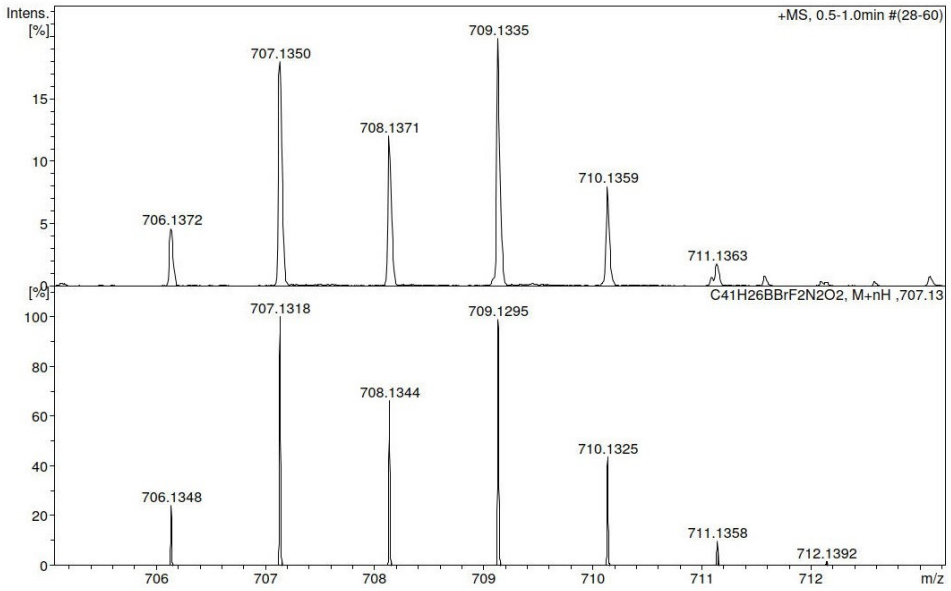

Bruker Compass DataAnalysis 4.0 printed: 03.05.2021 17:32:02 Page 1 of 1

4e

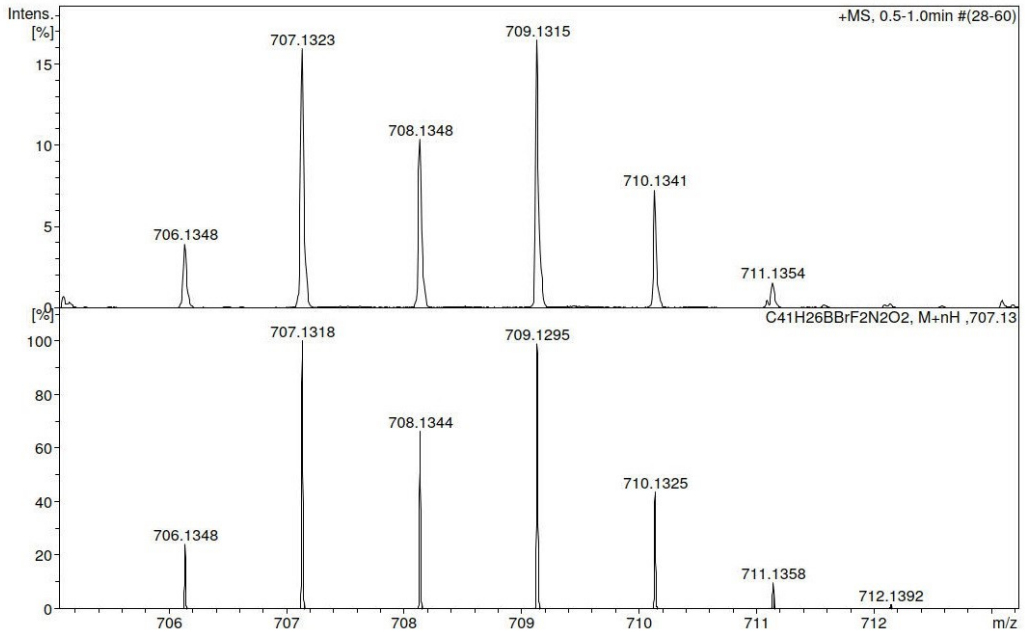

Bruker Compass DataAnalysis 4.0 printed: 03.05.2021 17:33:47 Page 1 of 1

4f

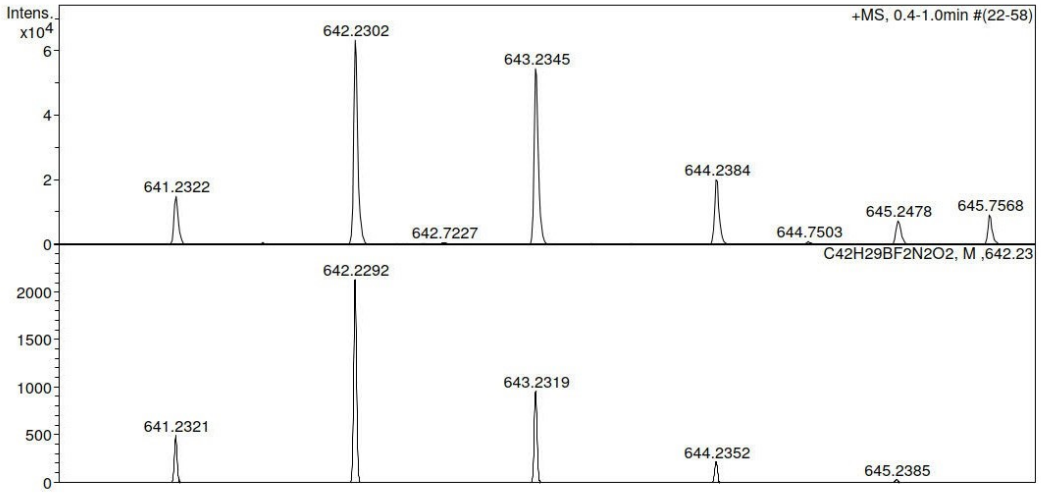

Bruker Compass DataAnalysis 4.0 printed: 06.12.2020 13:53:17 Page 1 of 1

4g

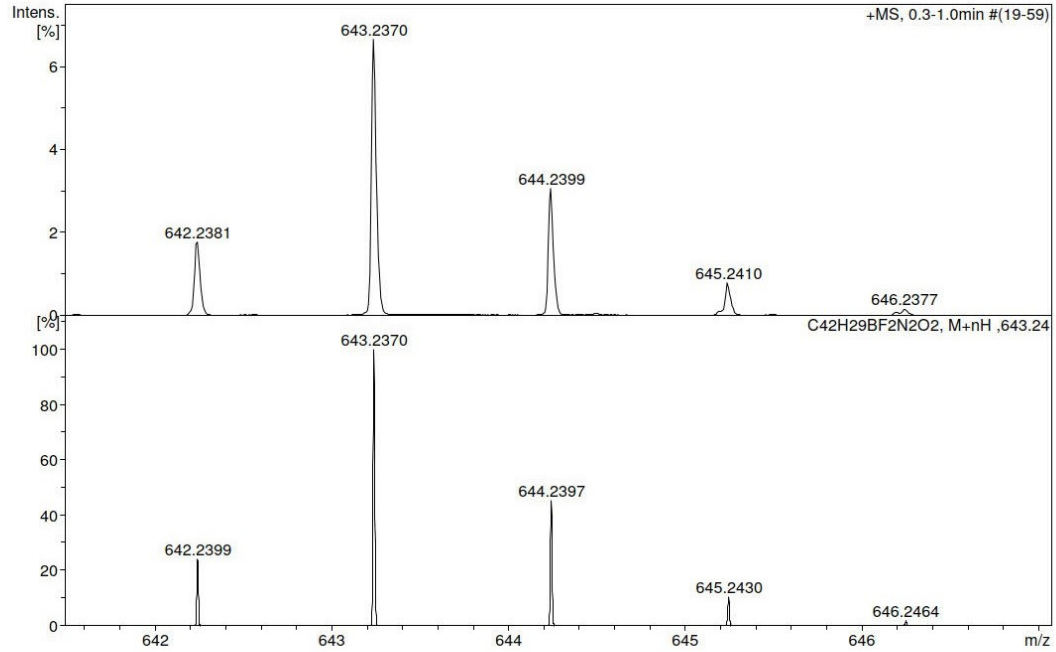

Bruker Compass DataAnalysis 4.0 printed: 03.05.2021 17:35:22 Page 1 of 1

4h

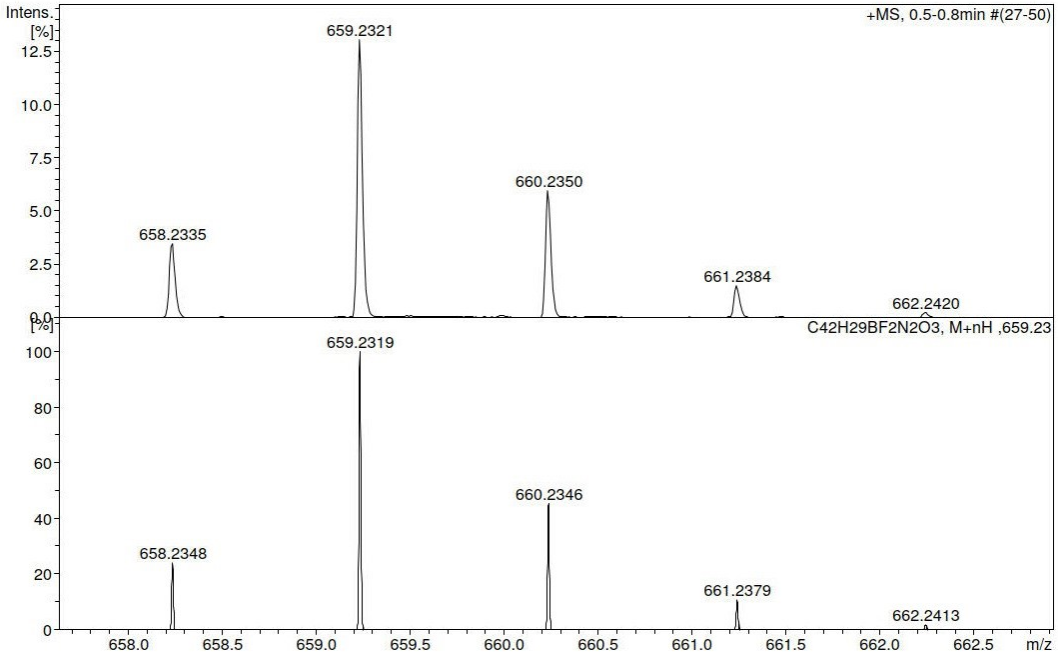

Bruker Compass DataAnalysis 4.0 printed: 03.05.2021 17:37:02 Page 1 of 1

4i

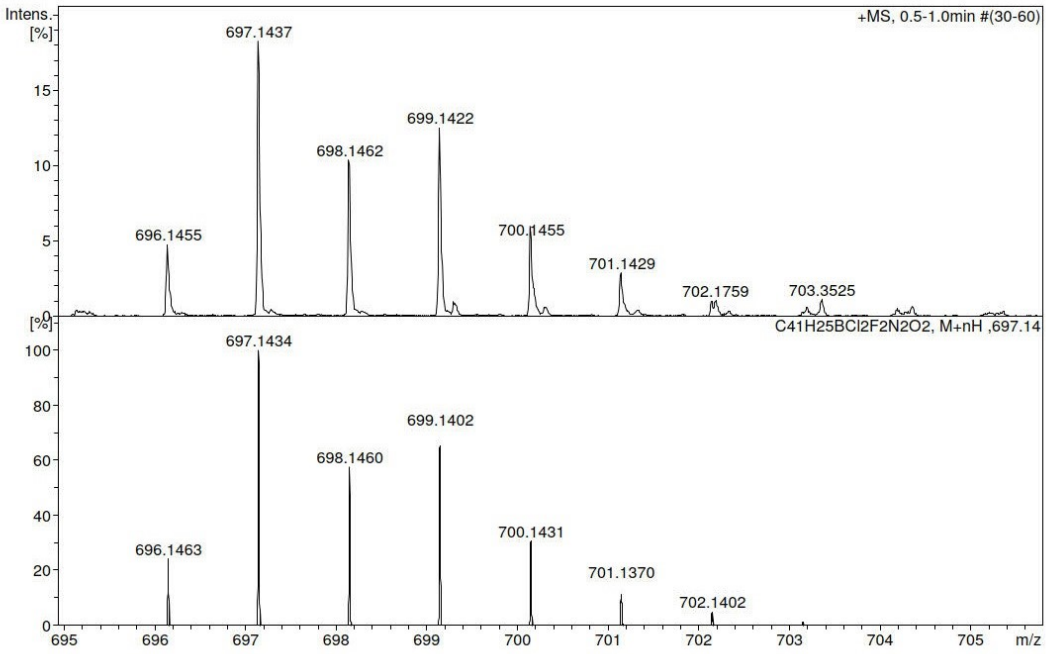
Intens.
[%]
+MS, 0.5-1.0min #(30-60)
697.1437
699.1422
698.1462
696.1455
700.1455
701.1429
702.1759
703.3525
C41H25BCl2F2N2O2, M+nH ,697.14
697.1434
699.1402
698.1460
696.1463
700.1431
701.1370
702.1402
695
696
697
698
699
700
701
702
703
704
705
m/z

4j

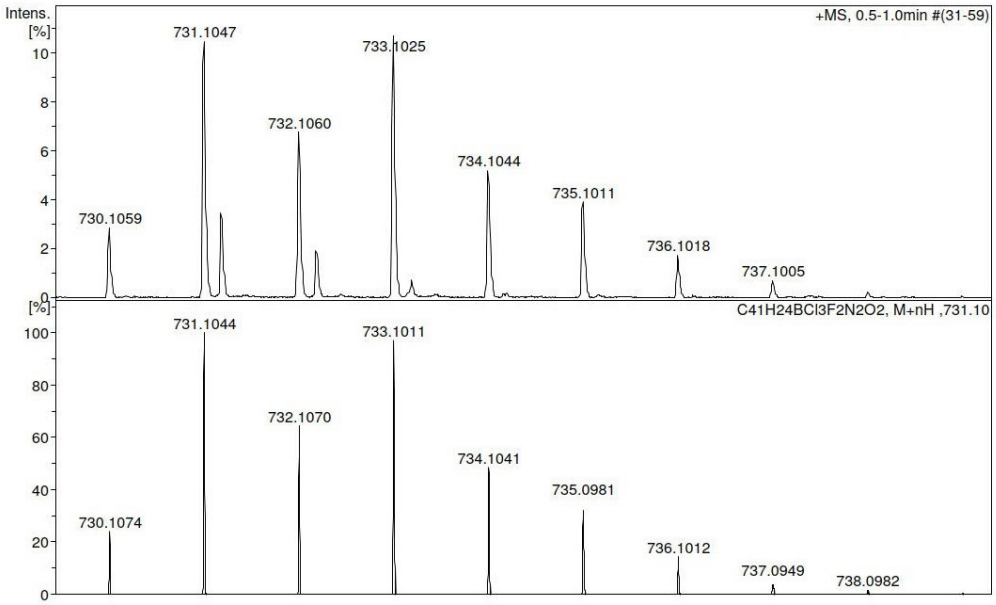
Intens.
[%]
+MS, 0.5-1.0min #(31-59)
731.1047
733.1025
732.1060
734.1044
735.1011
730.1059
736.1018
737.1005
C41H24BCl3F2N2O2, M+nH ,731.10
731.1044
733.1011
732.1070
734.1041
735.0981
730.1074
736.1012
737.0949
738.0982

4k

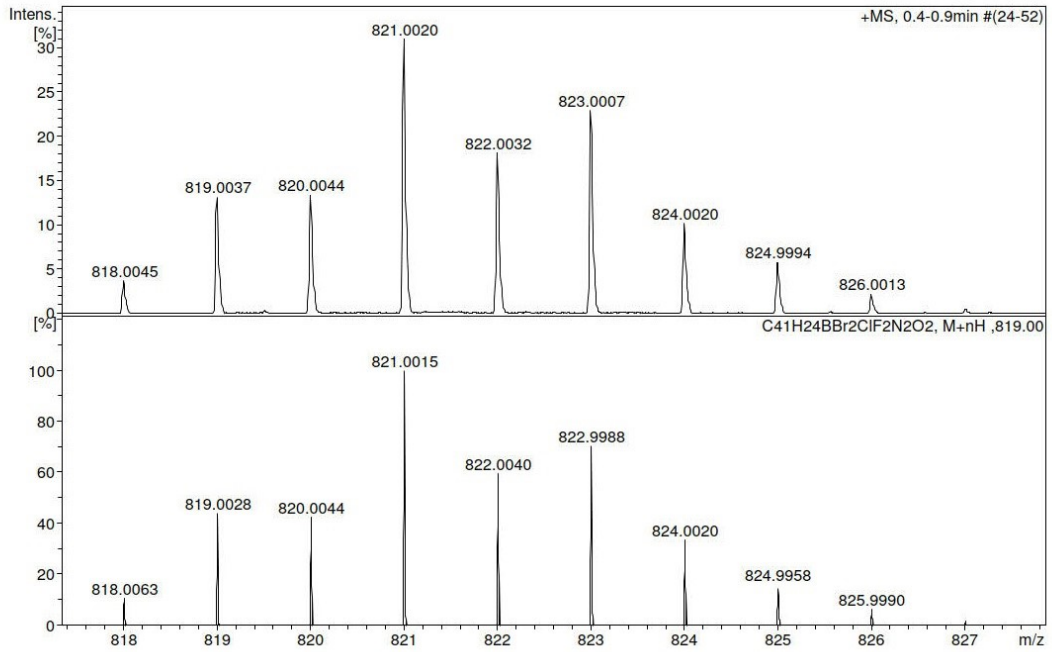

Bruker Compass DataAnalysis 4.0 printed: 03.05.2021 17:42:58 Page 1 of 1

4l

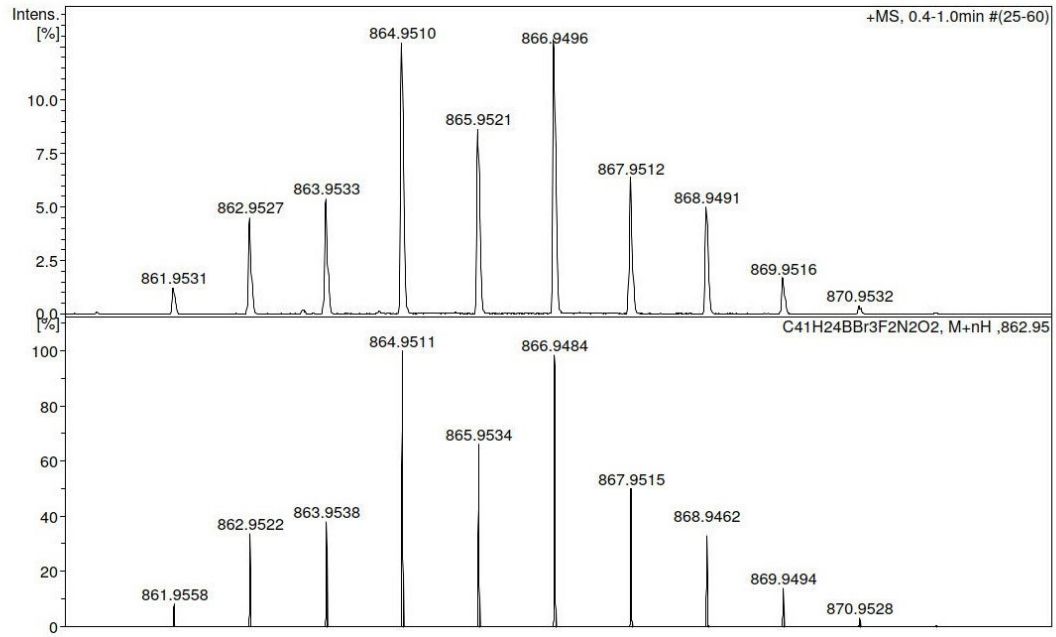

Bruker Compass DataAnalysis 4.0 printed: 03.05.2021 17:45:08 Page 1 of 1

4m

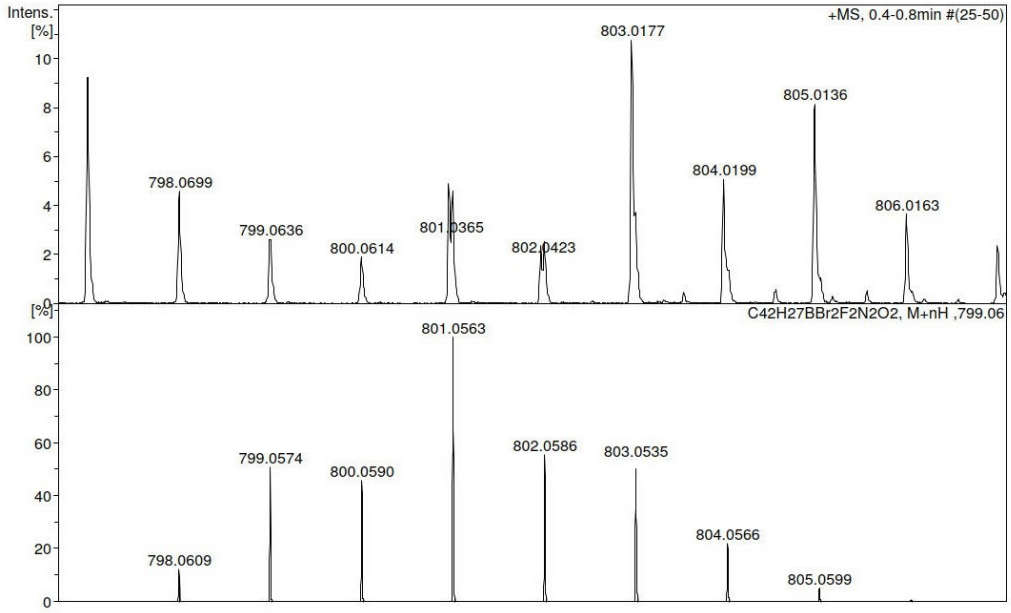

Bruker Compass DataAnalysis 4.0 printed: 03.05.2021 17:47:08 Page 1 of 1

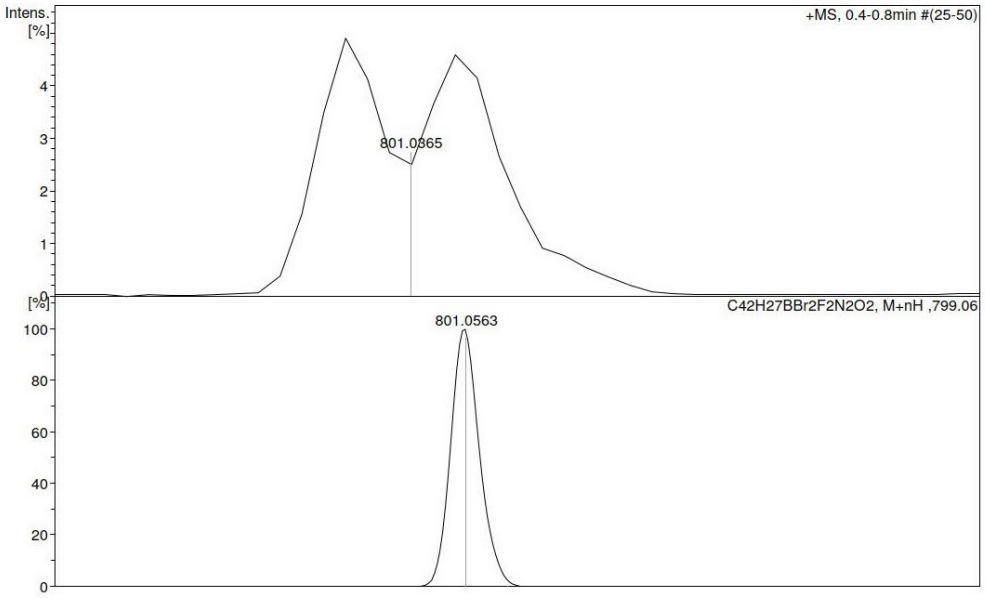

Bruker Compass DataAnalysis 4.0 printed: 03.05.2021 17:47:34 Page 1 of 1

4n

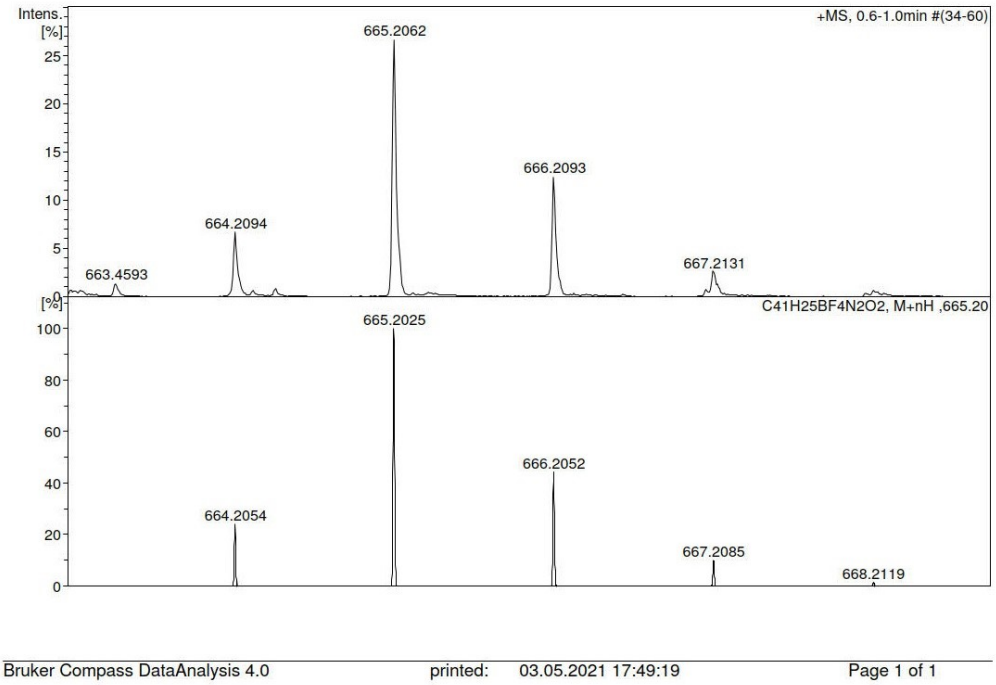

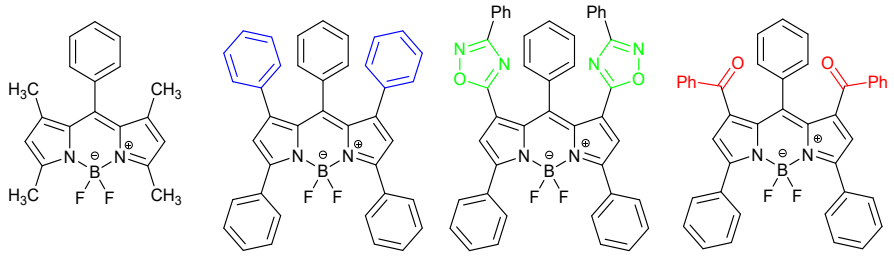

A	B	C	D
λ_{ex} = 501 nm λ_{em} = 513 nm QY = 0.63 (in DCM)	λ_{ex} = 561 nm λ_{em} = 597 nm QY = 0.31 (in THF)	λ_{ex} = 588 nm λ_{em} = 629 nm QY = 0.80 (in DCM)	λ_{ex} = 569 nm λ_{em} = 617 nm QY = 0.83 (in DCM)

Figure S1. Experimental variation of the main peaks for excitation (λ_{ex}) and emission (λ_{em}) in nm and quantum yield depending on BODIPY ligand variation.

3. Quantum-chemical calculations

DFT and time-dependent density functional theory (TD-DFT) calculations to obtain minimum energy structures in both the ground and excited states for all structures reported in the text were performed by using Gaussian16 set of programs.[1] The ground state was optimized at B3LYP level[2] with 6-31G(d,p) basis set and stationary points were characterized using vibrational analysis. The absorption spectra for all structures were simulated by using TD-DFT calculations with a range-separated versions CAM-B3LYP[3] and 6-311+G(d,p) basis set. Solvent effects were treated by the conductor-like polarizable continuum model (CPCM) model[4] adopted in the linear response formalism when used with TD-DFT. According to a general trend of TD-DFT

methods[5] we found an overestimation of calculated absorption band peaks with respect to the experimental ones (reported in Figure 4 for **4a**-**4n** structures and Figure 5 of the main text) of about 0.3 eV; nevertheless, the shift for absorption and emission spectra going from structures **A**-**D** of Figure S1 is well reproduced (Figure S2-A and Figure S2-B). Finally, our TD-DFT analysis revealed that the maximum of absorption for the $S_0 \leftarrow S_1$ transition corresponds to the HOMO and LUMO difference. The near-UV region with maximum at about 320-360 nm (see Figure S2-A) can be attributed to the $S_0 \leftarrow S_2$ and $S_0 \leftarrow S_3$ transitions and differences within the **4a**-**4n** structures may be found on the molecular contribution (compare Figure 6 and Figure S4). All details for the absorption and emission spectra for the new synthesized compounds are reported in Table S1 and Table S2. Finally, if we approximated the emission process by a vertical $S_0 \leftarrow S_1$ transition, the emission decay rate k_r from the excited to the ground state can be calculated by using the equation (1):

$$kr = \frac{4}{3}\frac{\Delta E3}{C3}\mu^2 10 \qquad (1)$$

where ΔE corresponds to the $S_0 \leftarrow S_1$ transition energy. c is the light speed and μ^2_{10} is the transition dipole strength calculated in atomic unit. The values used for the plot of Figure 9 of the main text are reported in Table S1 and Table S3.

Once calculated the k_r of equation (1) by using the computational values reported in Table S1 and Table S3, we can estimate the k_{nr} of selected BODIPY compounds by using the experimental quantum yield in the equation (2).

$$\Phi = k_r/(k_r+k_{nr}) \qquad (2)$$

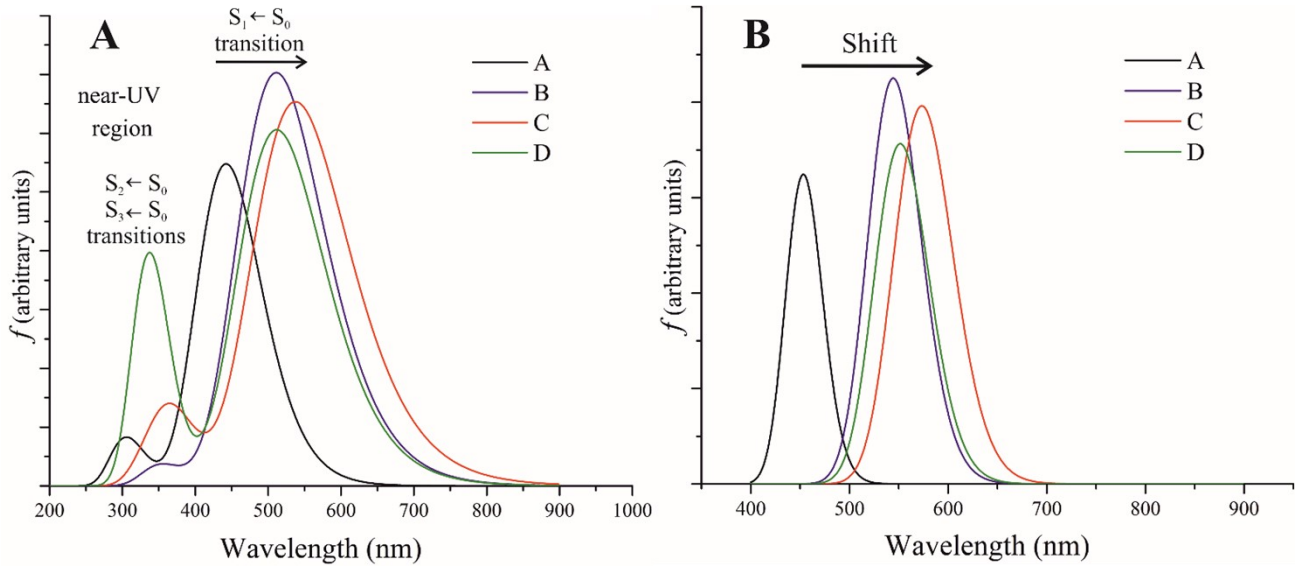

Figure S2 TD-DFT (CAM-B3LYP/6311+G(d,p)) simulated spectra for excitation (**A**) and emission (**B**) of BODIPY compounds (**A**, **B**, **C**, **D**) reported in Figure S1 in CH_2Cl_2 as solvent.

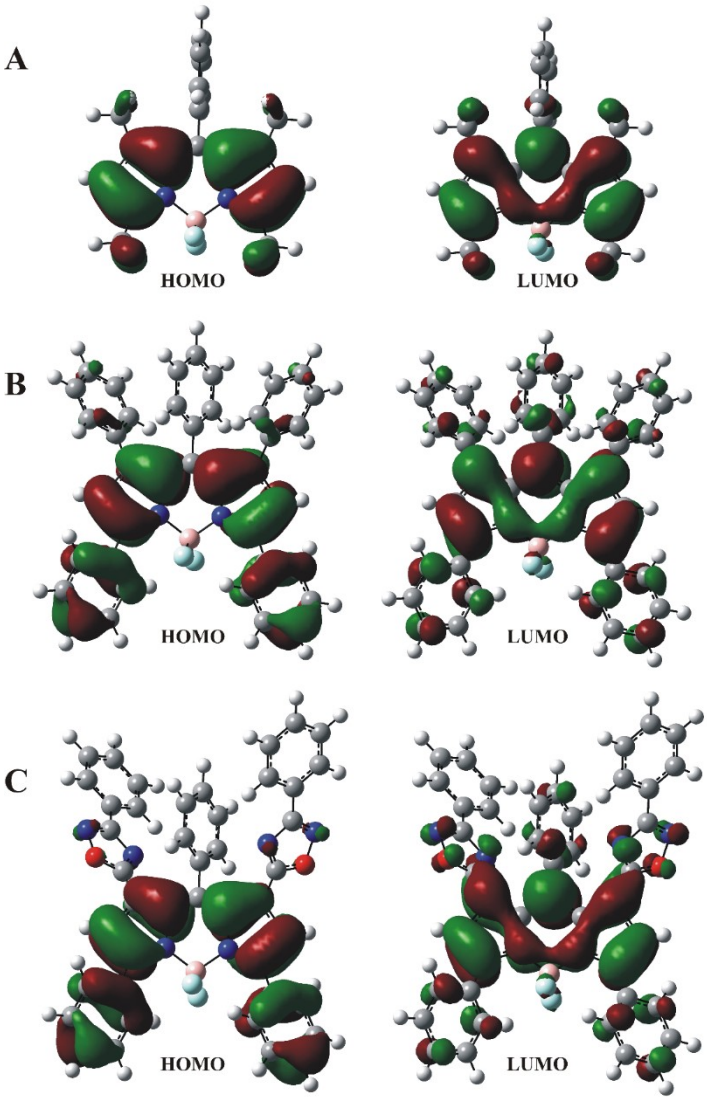

Figure S3. TD-DFT (CAM-B3LYP/6311+G(d,p)) molecular orbital for $S_0 \leftarrow S_1$ transition corresponding to the HOMO (left) and LUMO (right) difference for BODIPY compounds **A**, **B**, **C** reported in Figure S1 in CH_2Cl_2 as solvent.

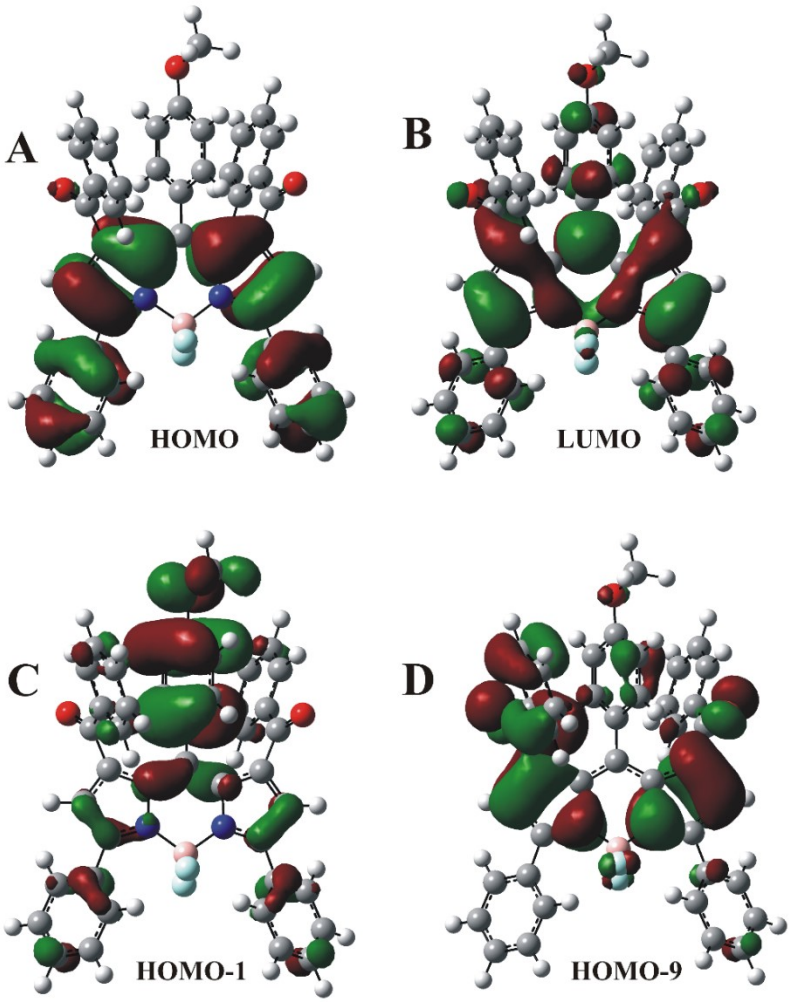

Figure S4. TD-DFT (CAM-B3LYP/6311+G(d,p)) molecular orbital of **4h** for the absorption peak at λ_{ex} 565 nm ($S_0 \leftarrow S_1$ transition) corresponding to the HOMO (**A**) and LUMO (**B**) difference whereas the maximum at about 325 nm can be attributed to the $S_0 \leftarrow S_2$ and $S_0 \leftarrow S_3$ transitions coming from the HOMO-1 (**C**) and HOMO-9 (**D**).

Table S1. Calculated main assignments (coefficient), excitation energies *E* (in eV), maximum absorption wavelengths λ_{abs} (in nm), the oscillator strength *f*, for selected compounds at the TD-CAM-B3LYP/6-311+G(d,p)//B3LYP/6-31G(d,p) level by using dichloromethane as solvent (CPCM).

Compounds	Main assignment	*E*	λ_{abs}	*f*
A	H → L (0.70017)	2.8029	442.34	0.6763
A	H_{-1} → L (0.6913)	3.8654	320.76	0.0474
A	H_{-2} → L (0.7003)	4.1668	297.55	0.0699
B	H → L (0.6965)	2.4287	510.49	0.8634
B	H_{-1} → L (0.6886)	3.3556	369.49	0.0039
B	H_{-11} → L (0.14859)	3.5117	353.06	0.0420
C	H → L (0.696)	2.3104	536.62	0.8027
C	H_{-1} → L (0.593)	3.3502	370.09	0.1473
C	H_{-10} → L (0.586)	3.7130	333.92	0.0476
D (4a)	H → L (0.69527)	2.4225	511.79	0.7480
D (4a)	H_{-1} → L (0.64369)	3.6673	338.08	0.4475
D (4a)	H_{-8} → L (0.49436)	3.7628	329.50	0.0450
4b	H → L (0.69534)	2.4161	513.16	0.7493
4b	H_{-1} → L (0.65414)	3.6333	341.24	0.4449
4b	H_{-8} → L (0.53123)	3.7625	329.52	0.0404
4c	H → L (0.69530)	2.4095	514.55	0.7504
4c	H_{-1} → L (0.66378)	3.6507	339.62	0.5053
4c	H_{-8} → L (0.49913)	3.7575	329.97	0.0450
4d	H → L (0.695)	2.4053	515.47	0.7516
4d	H_{-1} → L (0.6613)	3.6828	336.65	0.5226
4d	H_{-9} → L (0.45180)	3.7580	329.92	0.0577
4e	H → L (0.69617)	2.3130	536.02	0.8180
4e	H_{-1} → L (0.56361)	3.5521	349.05	0.0577
4e	H_{-1} → L (0.28836)	3.6880	336.19	0.0085
4f	H → L (0.69514)	2.4304	510.13	0.7411
4f	H_{-1} → L (0.67621)	3.4840	355.87	0.4413
4f	H_{-8} → L (0.44567)	3.7655	329.27	0.0287
4g	H → L (0.69571)	2.3806	520.81	0.8182
4g	H_{-1} → L (0.56147)	3.4482	359.57	0.0538
4g	H_{-2} → L (0.42078)	3.6972	335.35	0.0244
4h	H → L (0.69503)	2.4370	508.76	0.7319
4h	H_{-1} → L (0.68993)	3.2008	387.36	0.4135
4h	H_{-9} → L (0.47307)	3.7716	328.73	0.0289
4i	H → L (0.69503)	2.4115	514.13	0.7453
4i	H_{-1} → L (0.64179)	3.6627	338.51	0.4610
4i	H_{-9} → L (0.51749)	3.7637	329.42	0.0458
4j	H → L (0.69506)	2.3999	516.63	0.7486
4j	H_{-1} → L (0.66193)	3.6442	340.22	0.5185
4j	H_{-7} → L (0.46753)	3.7598	329.77	0.0452
4k	H → L (0.69505)	2.3936	517.99	0.7461
4k	H_{-1} → L (0.66115)	3.6373	340.87	0.5258
4k	H_{-7} → L (0.46402)	3.7576	329.96	0.0441
4l	H → L (0.69512)	2.3926	518.19	0.7480
4l	H_{-1} → L (0.66026)	3.6717	337.68	0.5453
4l	H_{-7} → L (0.47451)	3.7587	329.86	0.0554
4m	H → L (0.69540)	2.3652	524.19	0.8370
4m	H_{-1} → L (0.54808)	3.4290	361.57	0.0544
4m	H_{-2} → L (0.39946)	3.6823	336.71	0.0281
4n	H → L (0.69522)	2.4189	512.56	0.7485
4n	H_{-1} → L (0.64074)	3.6719	337.66	0.4618
4n	H_{-8} → L (0.52516)	3.7733	328.58	0.0444

Table S2. Calculated main assignments (coefficient), excitation energies *E* (in eV), maximum emission wavelengths λ_{em} (in nm), the oscillator strength *f*, for selected compounds at the TD-CAM-B3LYP/6-311+G(d,p)//TD-CAM-B3LYP/6-31G(d,p) level, by using dichloromethane as solvent (CPCM).

Compounds	Main assignment	*E*	λ_{em}	*f*
A	H ← L (0.7005)	2.7353	453.27	0.6400
B	H ← L (0.6977)	2.2775	545.26	0.8429
C	H ← L (0.6969)	2.1620	573.48	0.7815
D (4a)	H ← L (0.6964)	2.2477	551.61	0.7032
4b	H ← L (0.6949)	2.2445	552.40	0.7074
4c	H ← L (0.69646)	2.2337	555.07	0.7041
4d	H ← L (0.6965)	2.2288	556.28	0.7037
4e	H ← L (0.69740)	2.1230	584.01	0.7743
4f	H ← L (0.69627)	2.2604	548.50	0.7010
4g	H ← L (0.69687)	2.1662	572.37	0.7733
4g	H_{-1} ← L (0.64922)	3.1527	393.27	0.0851
4g	H_{-2} ← L (0.50807)	3.5145	352.78	0.0361
4h	H ← L (0.69621)	2.2703	546.11	0.6981
4h	H_{-1} ← L (0.69023)	3.0996	400.00	0.4309
4h	H_{-9} ← L (0.46426)	3.7015	334.95	0.0195
4i	H ← L (0.69621)	2.2371	554.23	0.6976
4j	H ← L (0.69626)	2.2232	557.68	0.6980
4k	H ← L (0.69626)	2.2179	559.02	0.6954
4l	H ← L (0.69632)	2.2150	559.74	0.6955
4m	H ← L (0.69622)	2.1533	575.78	0.7945
4n	H ← L (0.69635)	2.2450	552.27	0.7037

Table S3. Experimental QY and calculated TD-CAM-B3LYP/6-311+G(d,p) (dichloromethane as solvent (CPCM)) k_r, and k_{nr} values following the equations (2) and (3). The energies for the S_0 ← S_1transition are reported in Table S1.

Compounds	QY	k_{nr} (s^{-1})	k_{nr} (s^{-1})	μ^2_{10}
4a	0.83	$9.44(10^{-10})$	$4.60702(10^{-9})$	12.6022
4b	0.84	$8.71(10^{-10})$	$4.5706(10^{-9})$	12.6022
4c	0.96	$1.91(10^{-10})$	$4.57288(10^{-9})$	12.7124
4d	0.71	$1.86(10^{-9})$	$4.56422(10^{-9})$	12.7549
4f	0.67	$2.32(10^{-9})$	$4.7086(10^{-9})$	12.7549
4h	0.12	$3.35(10^{-8})$	$4.56228(10^{-9})$	12.2584

4. Reference

1 M. J. T. Frisch, G.W.; Schlegel, H.B.; Scuseria, G.E.; Robb, M.A.; Cheeseman, J.R.; Montgomery, Jr., J.A.; Vreven, T.; Kudin, K.N.; Burant, J.C.; Millam, J.M.; Iyengar, S.S.; Tomasi, J.; Barone, V.; Mennucci, B.; Cossi, M.; Scalmani, G.; Rega, N.; Petersson, G.A.; Nakatsuji, H.; Hada,M.; Ehara, M.; Toyota, K.; Fukuda, R.; Hasegawa, J.; Ishida, M.; Nakajima, T.; Honda, Y.; Kitao, O.; Nakai, H.; Klene, M.; Li, X.; Knox, J.E.; Hratchian, H.P.; Cross, J. B.; Bakken, V.; Adamo, C.; Jaramillo, J.; Gomperts, R.;Stratmann, R.E.; Yazyev, O.; Austin, A.J.; Cammi, R.; Pomelli, C.; Ochterski, J.W.; Ayala, P.Y.; Morokuma,K.; Voth, G.A.; Salvador, P.; Dannenberg, J.J.; Zakrzewski, V.G.; Dapprich, S.; Daniels, A.D.; Strain, M.C.;Farkas, O.; Malick, D.K.; Rabuck, A.D.; Raghavachari, K.; Foresman, J.B.; Ortiz, J.V.; Cui, Q.; Baboul, A.G.;Clifford, S.; Cioslowski, J.; Stefanov, B.B.; Liu, G.; Liashenko, A.; Piskorz, P.; Komaromi, I.; Martin, R.L.; Fox, D.J.; Keith, T.; Al-Laham, M.A.; Peng, C.Y.; Nanayakkara, A.; Challacombe, M.; Gill, P.M.W.; Johnson, B.;Chen, W.; Wong, M.W.; Gonzalez, C.; and Pople, J.A.; Gaussian, Inc., Wallingford CT, 2004, 2004.

2 a) A. D. Becke, *J. Chem. Phys.*, 1993, **98**, 1372-1377; b) A. D. Becke, *J. Chem. Phys.*, 1993, **98**, 5648; c) C. Lee, W. Yang and R. G. Parr, *Phys. Rev. B*, 1988, **37**, 785.

3 T. Yanai, D. P. Tew and N. C. Handy, *Chem. Phys. Lett.*, 2004, **393**, 51.

4 M. Cossi, N. Rega, G. Scalmani and V. Barone, *J. Comput. Chem.*, 2003, **24**, 669.

5 D. Jacquemin, E. A. Perpète, G. E. Scuseria, I. Ciofini and C. Adamo, *J. Chem. Theory Comput.*, 2008, **4**, 123.